The Chemokine Receptor CXCR3 Promotes CD8$^+$ T Cell Accumulation in Uninfected Salivary Glands but Is Not Necessary after Murine Cytomegalovirus Infection

Sofia Caldeira-Dantas,*,†,‡ Thomas Furmanak,* Corinne Smith,* Michael Quinn,* Leyla Y. Teos,§ Adam Ertel,¶ Drishya Kurup,* Mayank Tandon,§ Ilias Alevizos,§ and Christopher M. Snyder*

Recent work indicates that salivary glands are able to constitutively recruit CD8$^+$ T cells and retain them as tissue-resident memory T cells, independently of local infection, inflammation, or Ag. To understand the mechanisms supporting T cell recruitment to the salivary gland, we compared T cell migration to the salivary gland in mice that were infected or not with murine CMV (MCMV), a herpesvirus that infects the salivary gland and promotes the accumulation of salivary gland tissue-resident memory T cells. We found that acute MCMV infection increased rapid T cell recruitment to the salivary gland but that equal numbers of activated CD8$^+$ T cells eventually accumulated in infected and uninfected glands. T cell recruitment to uninfected salivary glands depended on chemokines and the integrin α_4. Several chemokines were expressed in the salivary glands of infected and uninfected mice, and many of these could promote the migration of MCMV-specific T cells in vitro. MCMV infection increased the expression of chemokines that interact with the receptors CXCR3 and CCR5, but neither receptor was needed for T cell recruitment to the salivary gland during MCMV infection. Unexpectedly, however, the chemokine receptor CXCR3 was critical for T cell accumulation in uninfected salivary glands. Together, these data suggest that CXCR3 and the integrin α_4 mediate T cell recruitment to uninfected salivary glands but that redundant mechanisms mediate T cell recruitment after MCMV infection. ***The Journal of Immunology*****, 2018, 200: 000–000.**

The salivary gland is an exocrine organ composed mostly of acinar cells producing a water-based fluid, which is rich is mucus, ions, and enzymes, that is released in the oral cavity via a network of epithelial ducts. Because of this, several viruses, including all human betaherpesviruses and gammaherpesviruses, infect the salivary gland and use saliva as a major route of transmission to new hosts (1–3). How the immune system responds to pathogens in the salivary gland and prevents or limits viral shedding remain poorly defined. In addition, how pathogens alter the salivary gland environment by infection is unknown.

CMV is a betaherpesvirus that infects most organs in the body but undergoes prolonged replication in the salivary gland. CMV infects the acinar and ductal epithelial cells in the salivary gland and, thus, is shed into saliva during replication (4–6). Using the mouse CMV (MCMV) model, it was shown >40 y ago that lymphocytes enter the salivary gland, resulting in the death of MCMV-infected epithelial cells (7, 8). MCMV also establishes latency in the salivary gland and readily reactivates in this tissue during periods of immune suppression, particularly when CD8$^+$ T cells have been depleted (9). It might be assumed that lymphocytes are drawn to the salivary gland in response to the CMV infection. Interestingly, however, recent data from several laboratories, including our own, suggested that Ag-stimulated CD8$^+$ T cells could be recruited to the salivary gland constitutively after MCMV infection or even without specific infection of the gland (10–12). MCMV-specific T cell populations were abundant in the salivary gland after MCMV infection where they adopted an intraepithelial localization and expressed CD69 and CD103 (10, 11), markers of tissue-resident memory T cells (T_{RM}). T_{RM} are memory T cell subsets that are retained in tissues independently of the circulating pool of T cells, thus providing a rapid defense against reactivation of a latent infection or local reinfection of a previously encountered pathogen (13, 14). Surprisingly, even in vitro–activated T cells could migrate to the salivary gland where they developed into protective T_{RM} in the complete absence of infection or specific inflammation (10–12), leading to the description of the salivary gland as a "sink" for CD8$^+$ T_{RM} (10).

*Department of Immunology and Microbiology, Thomas Jefferson University, Philadelphia, PA 19107; †Life and Health Sciences Research Institute (ICVS), School of Medicine, University of Minho, 4710-057 Braga, Portugal; ‡Life and Health Sciences Research Institute (ICVS)/3B's Associate Laboratory, 4710-057 Braga, Portugal; §Sjögren's Syndrome and Salivary Gland Dysfunction Unit, National Institute of Dental and Craniofacial Research, National Institutes of Health, Bethesda, MD 20892; and ¶Department of Cancer Biology, Sidney Kimmel Cancer Center, Thomas Jefferson University, Philadelphia, PA 19107

ORCIDs: 0000-0002-5467-4663 (S.C.-D.); 0000-0002-3804-3861 (T.F.); 0000-0001-6548-9802 (C.S.); 0000-0002-5854-6730 (L.Y.T.); 0000-0001-7455-1559 (A.E.); 0000-0002-3959-7700 (D.K.); 0000-0003-1370-7198 (C.M.S.).

Received for publication September 5, 2017. Accepted for publication November 17, 2017.

This work was supported by National Institutes of Health Grant AI106810 (to C.M.S.) and Portuguese Foundation for Science and Technology Grant SFRH-BD-52319-2013 (to S.C.-D.).

The gene expression data presented in this article have been submitted to the National Center for Biotechnology Information Gene Expression Omnibus (https://www.ncbi.nlm.nih.gov/geo/) under accession number GSE107338.

Address correspondence and reprint requests to Dr. Christopher M. Snyder, Thomas Jefferson University, Department of Microbiology and Immunology, Sidney Kimmel Cancer Center, 233 S. 10th Street, BLSB, Room 730, Philadelphia, PA 19107. E-mail address: christopher.snyder@jefferson.edu

The online version of this article contains supplemental material.

Abbreviations used in this article: B6, C57BL/6; FDR, false discovery rate; f.p., footpad; GSEA, Gene Set Enrichment Analysis; i.n, intranasal; I.V.$^+$, vasculature localized; I.V.$^-$, parenchyma localized; KO, knockout; LCMV-WE, lymphocytic choriomeningitis virus strain WE; MCMV, mouse CMV; PTx, pertussis toxin; RNA-Seq, RNA sequencing; RT-qPCR, reverse transcriptase quantitative PCR; T_{RM}, tissue-resident memory T cell; VACV, vaccinia virus; WT, wild-type.

It is unknown whether local inflammation or Ag can enhance the recruitment or retention of $CD8^+$ T_{RM} in the salivary gland. However, this ability of salivary glands to attract and retain protective numbers of $CD8^+$ T_{RM}, without a local infection or inflammation, is quite unexpected. In most other sites in the body, tissue-localized inflammation and/or Ag is critical for the efficient recruitment of T cells or their retention as T_{RM} (15–24). The best-studied example of the interplay among Ag, inflammation, and T_{RM} formation is the skin, where inflammation alone is sufficient to enable T cell egress from the blood and formation of T_{RM} phenotype cells (22). Interestingly, although infection at one skin site could lodge T cells at distant skin locations (23, 25), the efficiency was very poor without local inflammation, and local Ag enhanced the maintenance of T_{RM} populations and shaped the specificity of the cells that were retained (16, 23, 24). Thus, although Ag and inflammation within a particular skin site are not absolutely required for T_{RM} formation, they markedly enhance the number of protective T_{RM} that are established in the skin. Other tissues have been less well studied, but a similar theme is repeated. In the vaginal mucosa, $CD8^+$ T cell entry during HSV infection was poor unless $CD4^+$ T cells in the tissue promoted local chemokines in an IFN-γ–dependent manner (17). In the lungs, the formation and maintenance of protective numbers of T_{RM} after multiple infections, including MCMV, depended on Ag and infection of the lungs (26, 27). The brain is even more restrictive, requiring infection or Ag for any detectable T_{RM} formation (20). In fact, other than the salivary gland, only the small intestine has been described as permissive of T_{RM} formation and maintenance in an Ag and infection–independent manner (28). Thus, the salivary gland and the small intestine may be uniquely capable of recruiting and retaining T cells without any specific infection.

Although many studies have addressed the mechanisms of T cell recruitment to the intestine [e.g., (28–31)], very little is known about the mechanisms of T cell recruitment to the salivary gland. A recent study demonstrated that systemic inflammation could induce expression of the cellular adhesion molecule VCAM-1 on vascular endothelial cells in the salivary gland and that this boosted the recruitment of activated T cells via the integrin α_4 (32), which pairs with the β_1 integrin to form the ligand for VCAM-1. At first glance, this supports the notion that inflammation will enhance T cell recruitment to the salivary gland. However, T_{RM} formation and maintenance were not studied. Moreover, the chemokines that recruit T cells to the salivary gland remain undefined.

We examined $CD8^+$ T cell recruitment to the salivary gland in the presence or absence of active MCMV infection. Our data confirm and extend recent observations that uninfected salivary glands were permissive to the recruitment and retention of activated $CD8^+$ T cells in a manner dependent on the integrin α_4. Moreover, active MCMV infection of the salivary glands increased the rapid recruitment of activated T cells. Remarkably, however, inflammation induced by MCMV infection did not enhance the number of T_{RM} that were ultimately lodged in the salivary gland. Indeed, many chemokines abundantly expressed in the salivary gland of infected and uninfected mice could attract MCMV-specific T cells in vitro, including CXCL9 (monokine induced by IFN-γ) and CXCL10 (IFN-inducible 10 KDa protein), ligands for the receptor CXCR3. CXCR3 is a chemokine receptor that has been described to be important for $CD8^+$ T cell migration to a variety of tissues, typically in the context of inflammation and infection (33). Unexpectedly, we found that CXCR3 expression by T cells was critical for efficient T cell accumulation in the salivary gland in uninfected mice but was dispensable for their accumulation in the salivary gland during MCMV infection. These data establish a mechanism for the surprisingly efficient recruitment of activated T cells to the salivary gland, even after a completely irrelevant infection.

Materials and Methods

Mice and infections

All mice were purchased from The Jackson Laboratory and bred in-house. C57BL/6 (B6), B6.SJL-Ptprc^{a}Pepc^b/BoyJ (CD45.1), B6.PL-Thy1^a/CyJ (Thy1.1), and IFN-γ–knockout (KO) (B6.129S7-Ifng^{tm1Ts}/J) mice were used as recipients in the adoptive-transfer experiments and to assess chemokine expression in the salivary gland. OT-I transgenic mice [B6-Tg(TcraTcrb)1100Mjb/J] were bred with CD45.1 mice, CXCR3-KO mice (B6.129P2-Cxcr3tm1Dgen/J), and CCR5-KO mice (B6.129P2-Ccr5tm1Kuz/J) to generate congenic wild-type (WT) OT-Is, CXCR3-KO OT-Is, or CCR5-KO OT-Is T cells.

MCMV-K181 virus (kindly provided by Ed Mocarski) was used in Figs. 1–6. MCMV–SL8-015 or MCMV–K181–tfr–OVA (both referred to here as MCMV-OVA) have been described (34, 35) and were used to expand OT-I T cells prior to the secondary adoptive transfer in Fig. 4A and 4B and in Figs. 7 and 8A–D. Finally, MCMV-K181 was used in Fig. 8F. Infections were performed using 2×10^5 PFU and the i.p. route (100 μl per injection) in all experiments, with the exception of Fig. 1, in which some of the infections were performed via the intranasal (i.n.) or footpad (f.p.) route in a total volume of 20–25 μl per inoculation after anesthesia with isoflurane. MCMV-K181, MCMV-OVA, and MCMV–SL8-015 were produced as described (34, 36–38). All protocols were approved by the Thomas Jefferson University Institutional Animal Care and Use Committee.

Lymphocyte isolation and FACS staining

For all of the experiments, i.v. Ab injections were performed, as described in (39, 40) without perfusion, to distinguish between vasculature-localized ($I.V.^+$) and parenchyma-localized ($I.V.^-$) $CD8^+$ T cells. In brief, mice were injected i.v. with 3 μg of an anti-CD8α Ab (clone 53-6.7 conjugated to BV650 or BV421) 3 min before sacrifice. Blood was collected from the retro-orbital sinus or from the chest cavity, after cutting the pulmonary vein at sacrifice, and the organs were collected in media containing an unlabeled CD8α Ab (clone 53-6.7). Total $CD8^+$ T cells were identified by CD8β staining during the phenotypic analyses, as described below.

Lymphocytes from the blood, spleen, inguinal lymph nodes, submandibular salivary glands (referred to as "salivary glands" throughout), kidneys, and lungs were isolated, as described previously (40), with minimal modifications. Briefly the mucosal organs were minced using a gentleMACS Dissociator (Miltenyi Biotec) and incubated at 37°C for 1–1.5 h in digestion media containing 1 mg/ml collagenase type IV, 5 mM $CaCl_2$, 50 mg/ml DNase I, and 10% FBS in RPMI 1640. Salivary glands were suspended in 40% Percoll and overlaid on top of a 75% Percoll layer, whereas the kidneys and lungs were suspended in 40% Percoll. Suspensions were centrifuged at $600 \times g$ for 25–30 min, and the lymphocytes were collected from the 75/40 interface (salivary glands) or pellets (kidney and lung).

Phenotypic analyses of T cells were performed using the following Abs: CD8α (clone 53-6.7), CD8β (YTS156.7.7), CD69 (clone H1.2F3), CD103 (clone 2E7), CD44 (clone IM7), KLRG1 (clone 2F1), CXCR3 (clone CXCR3-173), CXCR4 (clone L276F12), CXCR6 (clone SA051D1), and CX3CR1 (clone SA011F11). OT-I T cells were identified by their congenic markers with CD45.1 (clone A20) and/or CD45.2 (clone 104) and by the TCR chains Vα2 (clone B20.1) and Vβ5 (clone MR9-4). In Fig. 9E (Exp.2), donor cells were also identified by the Thy1.2 marker (clone 30-H12). All Abs were purchased from BioLegend or BD Biosciences. All MHC-tetramers, loaded with peptides from M38, were provided by the National Institutes of Health Tetramer Core Facility (http://tetramer.yerkes.emory.edu/) and were used as described (41). A tetramer loaded with the B8R peptide derived from vaccinia virus (VACV) was used as a negative control for the tetramer staining following a MCMV infection. All samples were collected on a BD LSRFortessa or LSR II flow cytometer and analyzed using FlowJo software (TreeStar). The gating strategy is shown in Supplemental Fig. 1.

In vitro T cell activation and expansion

OT-I T cells were activated in vitro based on the protocol described (12), with modifications. Briefly, splenocytes from OT-I mice were harvested, and 4×10^6 cells per milliliter were cultured with 1 μg/ml SIINFEKL peptide for 2 d. On the second day, the cells were resuspended to 5×10^5 cells per milliliter and incubated with 0.03 U/ml IL-2 that was renewed every 2 d for a total of 4–5 d until the adoptive transfer.

Adoptive transfers

All of the adoptive transfers were performed via retro-orbital injections in a volume of 100 μl between congenic donor and recipient mice (differing in CD45.1/.2 or Thy1.1/1.2 expression).

In vitro–activated T cells. For the adoptive transfers in Figs. 2–4C, 8E, 8F, and 9 and Supplemental Fig. 2, in vitro–activated $CD8^+$ $CD44^+$ OT-I T cells were transferred to congenic naive recipients or recipients infected for 9 wk (Fig. 2) or 11 d (Fig. 3) with MCMV-K181 (lacking OVA). For treatment with pertussis toxin (PTx), OT-I T cells were suspended at a concentration of 1.5×10^7 cells per milliliter and treated or not with 50 ng/ml PTx (Sigma-Aldrich) for 1 h at 37˚C prior to transfer. In Fig. 8F, WT and CCR5-KO OT-I T cells were mixed and cotransferred to B6 mice that were previously infected with MCMV-K181 for 11 d. The mixture of donor cells was treated with anti-CXCR3 blocking Ab (clone CXCR3-173) or isotype-control Ab (polyclonal Armenian hamster IgG) at a concentration of 30 μg per 4×10^7 cells for 15 min. Recipient mice were also treated with the anti-CXCR3 Ab or isotype control (250 μg per mouse) via i.p. injections on day −2, day 0 (day of transfer), and day 2. Blocking Abs and isotype controls were purchased from Bio X Cell. The same approach was used in Fig. 9, but only WT OT-I T cells were transferred to naive recipients.

In vivo–activated T cells. For in vivo activation (Figs. 4A, 4B, 7, 8A–D), naive OT-I T cells were transferred into naive congenic recipients, followed by infection with MCMV expressing the cognate SIINFEKL peptide (MCMV–SL8-015 or K181–MCMV–OVA) 1–3 d after transfer. The number of cells transferred is indicated in each figure legend. In Fig. 4A and 4B, 5×10^4 OT-I T cells were transferred into congenic recipients to produce large numbers of OT-I T cells for a secondary transfer by day 5 postinfection. In this experiment, OT-I T cells were recovered from the spleen 5 d postinfection, treated for 30 min with 60 μg/ml anti-α_4 (clone PS/2), anti-$\alpha_4\beta_7$ (clone DATK32), or the respective isotype controls, and transferred to a new group of infection-matched or naive recipients. The recipients were treated on the day of the transfer with 300 μg of each Ab or isotype control via i.p. injection. Organs were collected 2 d after the secondary transfer, and the tissues were processed as described above.

Cell-proliferation assays

To assess proliferation of OT-I T cells in naive or MCMV-infected mice (Supplemental Fig. 2), OT-I T cells were labeled with a cell tracer dye (CellTrace Violet or CFSE), following the manufacturer's instructions, before the adoptive transfer. Briefly, cells were suspended at a concentration of 10^6 cells per milliliter and incubated with 5 μM CellTrace Violet for 20 min or were suspended at a concentration of 1×10^7 cells per milliliter and incubated with 1 μM CFSE for 10 min.

Transwell migration assays

For Transwell migration assays, $CD8^+$ T splenocytes were isolated from MCMV-K181–infected mice (7 d) using an EasySep biotin selection kit (STEMCELL Technologies) and biotinylated Abs against erythrocytes (Ter119), CD19 (6D5), NK1.1 (PK136), I-A/I-E (M5/114.15.2), and CD4 (GK1.4), following the manufacturer's protocol. Typically, $CD8^+$ T cells were 80–90% pure following this protocol. Purified cells were resuspended in RPMI 1640 media containing 2% BSA and 25 nM HEPES buffer (migration media) at a concentration of 5×10^6 cells per milliliter and were incubated for 1 h at 37˚C. Subsequently, 5×10^5 cells, in a total volume of 100 μl, were added to the upper chamber of a 6.5-mm Polycarbonate Transwell system (Corning) with a pore diameter of 5 μm. Chemokines (all from BioLegend) were diluted in migration media and added to the lower chamber at titrating concentrations in a total volume of 600 μl (three or four replicate wells per concentration). Control (media alone) samples, without chemokines in the lower chamber of the Transwell plates, were included on every plate to account for plate-to-plate variations in T cell migration. All tests were run in duplicate or triplicate on every plate. Chemokine concentrations shown in Fig. 6 represent the optimal migration over control (media alone) wells based on replicate titrations of each chemokine. Cells in the Transwell plates were incubated for 1.5 h at 37˚C. At the end of the incubation, 200 μl of cells from the bottom chamber were mixed with counting beads (CountBright Absolute Counting Beads; Invitrogen), whereas the remaining volume was used for FACS analyses of tetramer-binding cells. Cells were collected by flow cytometry, as above.

Reverse transcriptase quantitative PCR

For assessment of chemokine receptors expressed by T cells in Fig. 7C and 7D, OT-I T cells were transferred to B6 mice that were subsequently infected with MCMV–K181–OVA ($n = 3$ mice). Seven days postinfection, spleen and salivary glands were collected, and $CD8^+$ T cells were enriched using an EasySep biotin selection kit (STEMCELL Technologies), as described above for the Transwell assays. OT-I T cells were sorted based on the congenic markers CD45.1 and CD45.2. RNA was extracted from the sorted OT-I T cells (Fig. 7C, 7D) and whole salivary glands of naive B6 or IFN-γ–KO mice (Fig. 9F) using an RNeasy Mini Kit (QIAGEN), and cDNA was recovered using a High Capacity cDNA Reverse Transcription Kit (Applied Biosystems). In both cases, the β-actin and chemokine receptor transcripts expressed were detected on a StepOnePlus system (Applied Biosystems) using predesigned quantitative PCR assays (Integrated DNA Technologies) and FAM for detection. The relative concentration of chemokine receptors on these cells was determined by comparing the chemokine receptor signal with the β-actin signal for the same sample on the same plate; data are expressed as the $2^{-\Delta CT}$ value [e.g., $2^{-(\text{CT value for chemokine A} - \text{CT value internal reference control A})}$].

RNA sequencing

For the RNA sequencing (RNA-Seq) analysis, salivary glands were collected from naive mice or from mice that were infected with 2×10^5 PFU MCMV-K181 i.p. for 14 d, and RNA was obtained using a miRCURY RNA Isolation Kit Tissues (Exiqon).

RNA cleanup and depletion of ribosomal RNA for RNA-Seq analysis. Prior to cDNA library preparation, RNA samples were purified using RNA Clean & Concentrator (catalog number R1015; Zymo Research) and treated with DNase I to remove contaminating genomic DNA. Validation of RNA quality and concentration was determined using an RNA 6000 Pico Kit (catalog number 5067-1513; Agilent Technologies) for the 2100 Bioanalyzer instrument (Agilent Technologies). Four micrograms of total RNA per sample were used as input for the depletion of ribosomal RNA (RiboMinus kit, catalog number A15020; Ambion), yielding 6% recovery of input RNA, on average.

RNA-Seq library preparation and sequencing. Library preparation was performed using an Ion Total RNA Seq Kit v2 (Thermo Fisher Scientific), according to the manufacturer's protocol. The yield and size scatter of the cDNA libraries were evaluated using High Sensitivity DNA Chips (catalog number 5067-4626; Agilent Technologies) on a 2100 Bioanalyzer instrument. The barcoded cDNA libraries were diluted to a final concentration of 100 pM and used for template preparation on an Ion Chef System using an Ion PI Hi-Q Chef Kit (catalog number A27198; Thermo Fisher Scientific). Sequencing was performed on the Ion Proton Sequencer system using Ion PI Chip Kit v3 (catalog number A26771; both from Thermo Fisher Scientific). Sequenced data were preprocessed on an Ion Torrent server with Torrent Suite Software 4.4.3.

RNA-Seq data analysis. Ion Torrent single-end sequence reads were mapped to the mm10 genome using Ion Torrent Torrent Server TMAP aligner, version 4.4.11. Gene abundances were estimated by counting strand-specific reads using the Subread package featureCounts tool; reads with mapq of 0 or multiple mappings were filtered out (42). Reads overlapping more than one gene feature were not counted because the transcript of origin could not be confidently determined, as recommended by the Subread/featureCounts manual. Resulting read counts were then used to analyze differential expression between infected and uninfected samples using the DESeq2 package for R/Bioconductor, with default settings (43). For additional data exploration and visualization, reads per kilobase per million reads estimates were calculated from featureCounts results.

Gene Set Enrichment Analysis (GSEA) was also performed to identify up- and downregulated gene groups among available pathway and gene ontology annotations (44). Mouse gene symbols were converted to their human orthologs, obtained from MGI on March 3, 2017, for compatibility with GSEA. GSEA preranked analysis was performed using the list of available human orthologs, the DESeq2 test statistic as the ranking metric, and GSEA enrichment score set to "classic," as described in the GSEA FAQ.

The sequencing data have been submitted to the National Center for Biotechnology Information Gene Expression Omnibus (https://www.ncbi.nlm.nih.gov/geo/) under accession number GSE107338.

ELISAs for chemokine expression

Whole salivary glands of naive B6 and IFN-γ–KO mice were collected in PBS with 10 μl/ml Halt Protease Inhibitor Cocktail (Thermo Fisher Scientific) and homogenized for two 30-s cycles in a mini bead beater. After centrifugation (14,000 × *g* for 15 min), the supernatant was stored at −80˚C. The total protein concentration was determined using a Quick Start Bradford Protein Assay (Bio-Rad). Samples were normalized to 8 mg/ml total protein. The concentration of CXCL9 in each sample was quantified

in duplicate using a CXCL9 (MIG) ELISA kit (Thermo Fisher Scientific), according to the manufacturer's specifications.

Statistical analysis

Differences in absolute numbers were determined after $\log_{10}$ transformation, and the fold change was determined based on the ratios of the geometric mean. The specific statistical test used for each experiment is indicated in the figure legends. Prism 6 for Mac OS X was used to determine the $\log_{10}$-transformed values and geometric mean, as well as to perform the statistical analysis.

Results

The route of MCMV infection impacts CD8$^+$ T cell migration to the salivary gland but not the rate of T_{RM} differentiation

We have previously shown that MCMV infection by the i.p. route led to robust formation of T_{RM} in the salivary gland postinfection (11). However, factors outside of the tissue, such as the site of T cell priming, may influence CD8$^+$ T cell trafficking and T_{RM} formation in some tissues (45–48). To determine whether the route of MCMV infection influenced the migration of CD8$^+$ T cells and the formation of MCMV-specific T_{RM}, we compared T_{RM} numbers 14 d postinfection via the i.p., i.n., and f.p. routes. In this experiment, and throughout, cells that were still within the circulation were distinguished from those that had reached the parenchyma by intravascular staining with anti-CD8 Abs, as described in *Materials and Methods*. As shown in Fig. 1, MCMV-specific T cells reached the parenchyma of the salivary gland after all three routes of infection and developed the T_{RM} phenotype. Interestingly, infections by the i.n. and f.p. routes were associated with lower overall numbers of MCMV-specific T cells in the salivary gland, which reached statistical significance after f.p. infection. Notably, this effect was not due to an overall difference between circulating populations, as reflected by the similar number of MCMV-specific T cells in the spleen at the same time point after all three infections. Importantly, however, the frequency of T cells that developed the T_{RM} phenotype in the salivary gland was identical after all three routes of infection (Fig. 1C), implying that once T cells arrived in the gland, they were equally capable of differentiating into T_{RM}. In contrast, MCMV-specific T_{RM} only formed in the lung after i.n. infection (Fig. 1B, 1C), which confirms the results of a recent study (19). These data suggest that the route of infection impacts the ability of T cells to reach the salivary gland but not their differentiation into T_{RM}.

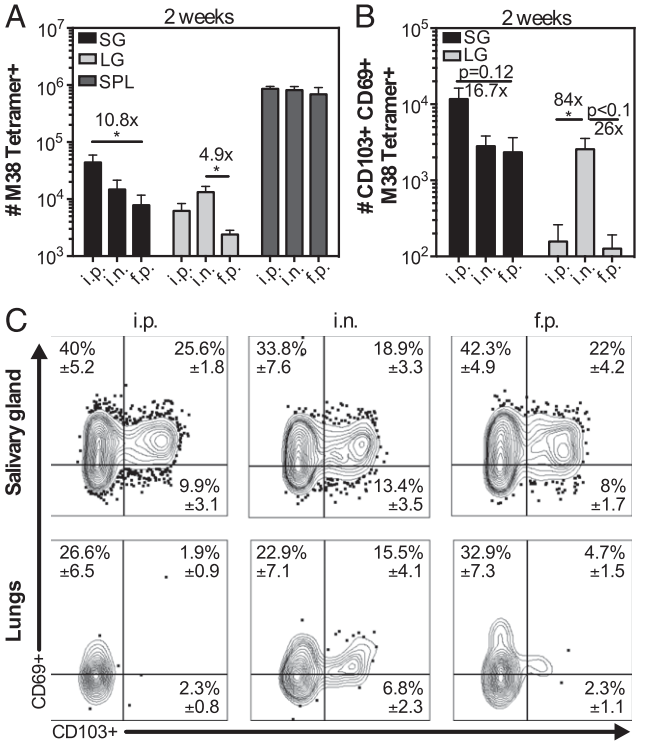

FIGURE 1. MCMV-specific CD8$^+$ T cells accumulate in the salivary gland after several routes of MCMV infection. Mice were infected by i.p., i.n., and f.p. inoculation. Cells in the parenchyma or vasculature of each tissue were distinguished by i.v. staining, as described in *Materials and Methods*. (**A**) Absolute number of M38 tetramer$^+$ CD8$^+$ T cells from the parenchyma of the salivary gland (SG) and lungs (LG) and from the overall CD8β$^+$ population of the spleen (SPL) 2 wk postinfection. (**B**) Absolute number of CD103$^+$ CD69$^+$ M38 Tetramer$^+$ cells in the SG and LG from the data shown in (A). Data are from two independent experiments ($n = 6$ for f.p. and i.p.; $n = 5$ for i.n.). Error bars represent the SEM. (**C**) Concatenated FACS plots from one representative experiment ($n = 2$ for i.n.; $n = 3$ for i.p. and f.p.) of CD69 and CD103 expression of M38 Tetramer$^+$ CD8$^+$ T cells from the salivary gland (upper panels) and the lungs (lower panel). The mean frequency ± SEM in the indicated quadrant were calculated considering both experiments. $*p < 0.05$, one-way ANOVA after $\log_{10}$ transformation of the absolute numbers.

Activated CD8$^+$ T cells can enter the salivary gland and develop the T_{RM} phenotype even when a pre-established T_{RM} population is already present

Previous studies suggested that activated T cells could enter and reside in naive uninfected salivary glands. Moreover, we previously suggested that persistent MCMV infection resulted in continuous recruitment and retention of new MCMV-specific T_{RM}, long after the primary infection had been resolved (11). To directly compare these two conditions, we activated OT-I T cells in vitro and transferred them to congenic mice that were naive or latently infected with WT MCMV lacking OVA (9 wk postinfection, Fig. 2A). WT MCMV was used in these experiments to assess the impact of viral infection and the presence of unrelated T_{RM}, as well as to avoid the complication of Ag-driven T cell expansion of the donor OT-I T cells. Two weeks after transfer, OT-I T cells had reached the salivary gland in similar numbers in naive and latently infected recipients (Fig. 2B), and similar frequencies of OT-I T cells expressing CD69 and CD103, the markers of bona fide T_{RM}, were observed in naive and infected salivary glands (Fig. 2C, 2D). Likewise, when naive or MCMV-infected mice were infected with VACV, VACV-specific T_{RM} (B8R tetramer$^+$) were present in the salivary glands in similar numbers, and the frequency of T_{RM}-phenotype VACV-specific T cells was equivalent between groups (data not shown). Thus, our data suggest that naive, acutely infected, and latently infected salivary glands are all capable of recruiting activated CD8$^+$ T cells and supporting their differentiation into T_{RM}.

Acute MCMV infection promotes rapid CD8$^+$ T cell recruitment to the salivary gland but does not affect the overall numbers of T_{RM}-phenotype T cells

Although the above experiments demonstrate that infection and inflammation are not needed for T cell recruitment to the salivary gland and development of the T_{RM} phenotype, MCMV infects the salivary gland directly, and our data do not exclude a role for acute inflammation in promoting the process. To directly compare T cell migration to naive salivary glands and salivary glands with active MCMV replication, in vitro–activated OT-I T cells were transferred to naive mice or mice infected 11 d previously with MCMV (Fig. 3), a time when replicating MCMV can be detected in the salivary glands after i.p. infection (11). For these experiments, we infected mice with WT MCMV (lacking OVA) to test the role of inflammation in the gland, again without the confounding issue of

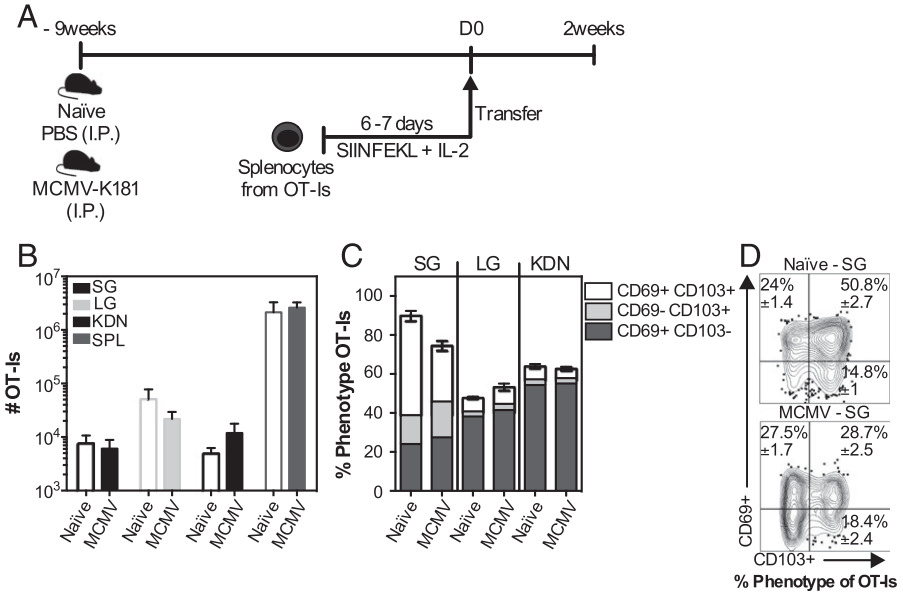

FIGURE 2. CD8$^+$ T cells with a T_{RM} phenotype can form in the salivary glands of naive mice and mice latently infected with MCMV. (**A**) Schematic diagram of the experimental design. Naive mice or mice that had been infected (i.p.) for 9 wk with WT MCMV (lacking OVA) were seeded with 3×10^6 in vitro–activated OT-I T cells and sacrificed 2 wk after transfer. (**B**) Absolute number of OT-I T cells from the parenchyma of the salivary gland (SG), lungs (LG), and kidneys (KDN) and from the overall CD8β$^+$ population of the spleen (SPL). (**C**) Frequency of CD103 and CD69 expression on OT-I T cells from the parenchyma of the SG, LG, and KDN. Data are combined from two independent experiments (n = 7). (**D**) Concatenated FACS plots from a representative experiment with frequency (mean ± SEM) values considering all of the experiments. An unpaired t test was used to test for statistical significance between infected and naive mice within each organ. No significant differences were found.

the transferred cells undergoing Ag-driven proliferation in infected mice. An increased recruitment of OT-I T cells to the salivary gland, but not other organs, was observed in the infected recipients early after transfer (Fig. 3B), which was not due to higher T cell proliferation rates in the infected glands (Supplemental Fig. 2). At later time points (31 d after transfer), there was a reduction in the number of OT-I T cells in the lung and the kidneys, as expected, due to the lack of Ag, but not in the salivary gland. Remarkably, the early advantage in

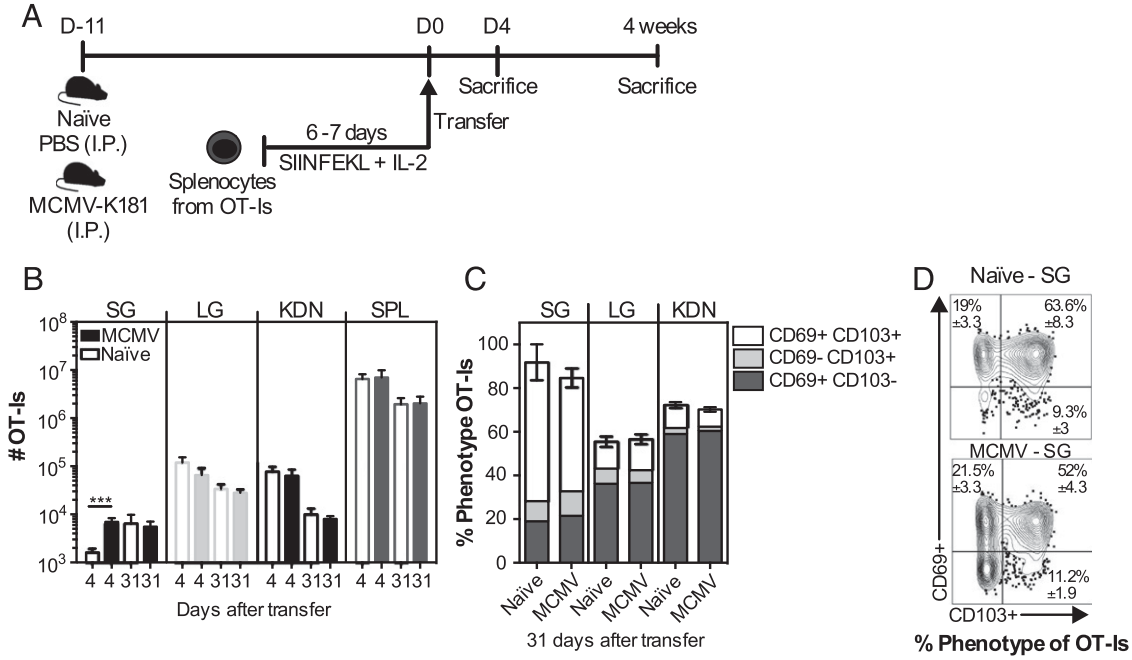

FIGURE 3. CD8$^+$ T_{RM}-phenotype cells can form and persist at similar numbers in salivary glands from MCMV-infected and naive mice. (**A**) Schematic diagram of the experimental design. Naive mice or mice infected i.p. 11 d earlier with MCMV were seeded with 3×10^6 in vitro–activated OT-I T cells. The recipients were sacrificed at 4 and 31 d after transfer. (**B**) Absolute number of OT-I T cells in the parenchyma of the salivary gland (SG), lung (LG), and kidney (KDN) and from the CD8β$^+$ cells of the spleen (SPL). (**C** and **D**) Frequency of CD103- and CD69-expressing OT-I T cells in the parenchyma of the SG, LG, and KDN at 31 d after transfer. Data are combined from two experiments (n = 7 naive and n = 6 infected recipients at day 4, n = 6 naive and n = 6 infected at day 31). (D) Concatenated FACS plots of CD103 and CD69 expression of OT-I T cells in the SG from one representative experiment (n = 3 naive and n = 3 infected recipients), with mean ± SEM values considering all of the experiments. Error bars represent SEM. ***$p < 0.001$, unpaired t test after $\log_{10}$ transformation of absolute numbers.

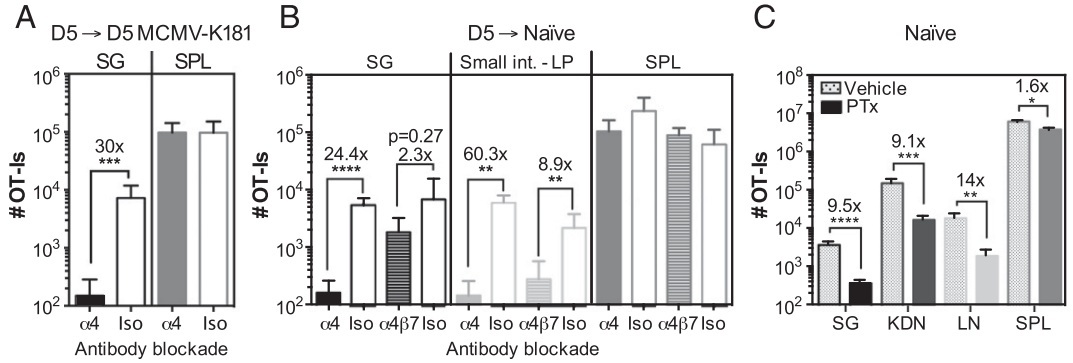

FIGURE 4. CD8$^+$ T cell accumulation in infected and uninfected salivary glands is dependent on α_4 integrin and chemokines. (**A** and **B**) Naive OT-I T cells (5×10^4) were transferred into congenic mice that were infected 1 d later with MCMV expressing OVA via the i.p. route. Splenocytes containing expanded OT-I T cells were recovered from the spleen 5 d later and transferred to mice infected with WT MCMV (lacking OVA) (A) or naive mice (B). Recipients were treated or not with anti-α4 blocking Ab on the day of the transfer, and mice were sacrificed 2 d after the transfer. Data show the absolute number of OT-I T cells recovered from the parenchyma of the salivary gland (SG) and the small intestine lamina propria (LP), as well as from the overall CD8β$^+$ fraction of the spleen (SPL). Results were combined from two independent experiments ($n = 5$ or 6 mice per group). (**C**) Naive B6 mice were seeded with 8×10^6 in vitro–activated OT-I T cells that had been treated with PTx or vehicle as a control before the adoptive transfer. Shown are the absolute numbers of OT-I T cells recovered from the parenchyma of the SG, kidneys (KDN), and lymph nodes (LN), as well as from the overall CD8β$^+$ T cell population of the SPL 4 d after the adoptive transfer. Results from two independent experiments were combined ($n = 7$). Error bars represent the SEM. $^*p < 0.05$, $^{**}p < 0.01$, $^{***}p < 0.001$, $^{****}p < 0.0001$, unpaired t test after $\log_{10}$ conversion of the absolute numbers.

T cell numbers recruited to the infected salivary gland was no longer evident (Fig. 3B). Moreover, the frequency of OT-I T_{RM} present in the salivary gland was similar in infected and naive recipients 31 d after transfer (Fig. 3C, 3D). Thus, surprisingly, our data suggest that, although inflammation of the salivary gland caused by MCMV infection resulted in an accelerated accumulation of activated OT-I T cells in the gland shortly after transfer, infection and inflammation provided no long-term advantage for the formation or maintenance of CD8$^+$ T_{RM}.

CD8$^+$ T cell homing to the salivary gland is mediated by $\alpha_4\beta_1$ and chemokines at steady-state

Recent data from Woyciechowski et al. (32) have suggested that the integrin $\alpha_4\beta_1$ plays a critical role in T cell recruitment to the salivary gland during systemic inflammation induced by i.v. polyinosinic-polycytidylic acid treatment. We wondered whether this mechanism would also contribute to T cell recruitment to naive salivary glands. To test this, naive WT OT-I T cells were transferred into congenic mice and driven to expand with MCMV-OVA infection. Five days postinfection, splenic T cells containing activated OT-I T cells were transferred to MCMV-K181 infection–matched or naive recipients in the presence or absence of Abs to block α_4 integrin or $\alpha_4\beta_7$ integrin. As expected, α_4 blockade greatly reduced the number of OT-I T cells in the salivary gland of infected recipients 2 d after transfer (Fig. 4A) (32). Likewise, in naive recipients, α_4 blockade reduced the numbers of OT-I T cells in the salivary gland and in the lamina propria of the small intestine compared with the group that received the isotype-control Ab; these differences were not observed in the spleens of the same animals (Fig. 4B). In contrast, the blockade of $\alpha_4\beta_7$ had no significant impact on T cells in the salivary gland, despite inhibiting OT-I T cell migration to the lamina propria of the small intestine (Fig. 4B), as expected (30, 32, 49). In addition, preincubation of OT-I T cells with retinoic acid, which strongly induces the $\alpha_4\beta_7$ integrin (50), had no effect on salivary gland migration (data not shown). The α_4 integrin is known to pair with the β_1 or β_7 chain. Therefore, these data suggest that $\alpha_4\beta_1$ is important for the migration of activated CD8$^+$ T cells to the salivary gland, regardless of infection. These data also imply that the salivary gland expresses sufficient VCAM-1, the ligand for $\alpha_4\beta_1$, independently of local MCMV infection.

Chemokines are important for activating integrins and promoting lymphocyte transendothelial migration. However, several recent reports have implicated chemokine-independent mechanisms of T cell recruitment (e.g., CD44, IL-33, or Ag) (51–53). To test whether chemokines are mediators of CD8$^+$ T cell recruitment to the naive salivary gland, OT-I T cells were activated in vitro and treated or not with PTx, which irreversibly inhibits signaling through G protein–coupled receptors like chemokine receptors (54–56). Untreated activated OT-I T cells migrated into all organs, including the salivary gland, within 4 d of transfer, as expected (Fig. 4C). In contrast, PTx treatment substantially reduced the numbers of OT-I T cells that migrated into the lymph nodes (Fig. 4C), as previously shown (55, 56), as well as the salivary gland and kidney (Fig. 4C). These data suggest that activated CD8$^+$ T cells migrate to naive salivary glands in response to a chemokine signal.

Chemokines expressed in the salivary gland with or without MCMV infection

To explore the chemokines expressed by the salivary gland in the presence or absence of MCMV infection, we used RNA-Seq. Salivary glands were extracted from naive mice or mice that had been infected for 2 wk with MCMV strain K181. Perhaps not surprisingly, the dominant changes in overall gene expression could be traced back to immune responses, type I IFN, and IFN-γ, including increases in genes encoding MHC molecules and Ag-processing machinery, Stat1, Stat2, Irf1, Irf7, and Ifitm3 (Supplemental Table IA, which shows all genes that increased or decreased significantly). Interestingly, a number of IFN-γ–induced guanylate-binding proteins (Gbp2, Gbp3, Gbp6, Gbp7, and Ifi47) and IFN-γ–induced GTPases (Iigp1, Irgm1, Irgm2, and Igtp) were among the most increased genes postinfection, suggesting a dominant IFN-induced change in gene expression. GSEA using the Gene Ontology Biological Process database revealed that the top 20 enriched gene sets were all related to innate and adaptive immune responses, cytokine signaling, type I IFN, IFN-γ, and leukocyte activation (Supplemental Table IC). In contrast, very few genes were significantly downregulated after MCMV infection (Supplemental Table IA). There were no significant changes in expression of integrins or cell adhesion molecules that survived correction for multiple testing errors (false discovery rate [FDR]

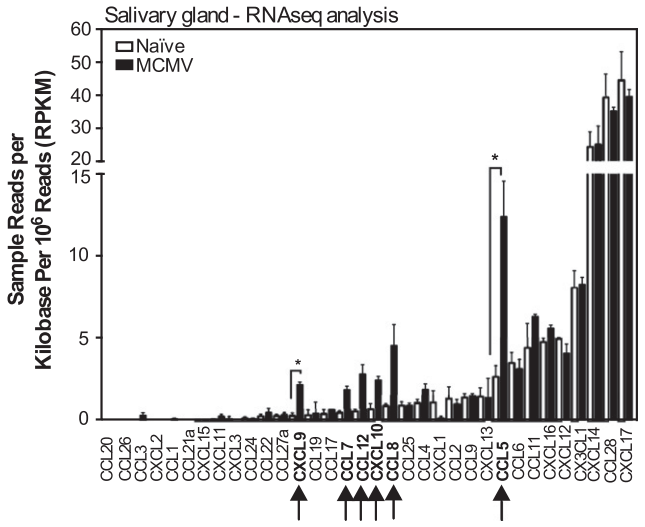

FIGURE 5. Chemokine profile of the salivary gland after MCMV infection. The array of chemokines expressed in the salivary glands of uninfected mice or mice 14 d after MCMV infection. Shown are the sample reads per kilobase per million reads (RPKM) of chemokines to illustrate the relative abundance of different transcripts. The complete list of genes that were significantly differentially expressed is shown in Supplemental Table IA. The complete gene list sorted by fold change, regardless of significance, is shown in Supplemental Table IB. Data are from one experiment ($n = 3$ mice per group). Error bars represent the SEM. $\uparrow p < 0.05$, *FDR < 0.05.

< 0.05), although expression of the α_4, α_L (CD11a), α_X (CD11c), and β_2 integrins was increased in the infected salivary glands when the gene set was filtered by a raw p value < 0.05 (Supplemental Table IB, which shows all genes, regardless of significance).

Of the chemokines, expression of CCL5 and CXCL9 was significantly increased by infection (FDR < 0.05) and CCL7, CCL8, CCL12, and CXCL10 were also detected when we used a raw p value cutoff of 0.05 (Fig. 5, Supplemental Table IA, IB). In contrast, several chemokines were abundantly expressed in the salivary gland, regardless of infection, including CCL28, CXCL12, CXCL14, CXCL16, CXCL17, and CX3CL1 (Fig. 5, Supplemental Table IB). All of these chemokines, with the exception of CXCL17, have been described to recruit T cells in various settings (29, 57–69). These data show that MCMV infection of the salivary gland induces a dominant inflammatory response centered on IFN-stimulated gene expression. However, several chemokines were abundantly expressed in the salivary gland, regardless of infection.

MCMV-specific T cells express multiple chemokine receptors and are able to migrate toward multiple chemokines

To test whether MCMV-specific T cells could migrate to some of the chemokines that were present in the salivary gland independently of infection, we conducted Transwell migration assays in vitro with the top six most abundantly expressed chemokines, along with CCL5, CXCL9, CXCL10, and CCL19. T cells were harvested from the spleens of mice 7 d after MCMV infection, which represents the peak of T cell clonal expansion (34, 70) and a time at which splenic T cells migrate readily to the salivary gland in adoptive-transfer experiments (data not shown). In multiple experiments, CCL28 and CXCL16 failed to induce any migration of splenic $CD8^+$ T cells (data not shown). In contrast, robust $CD8^+$ T cell migration was induced by CCL19 (~9-fold increased over background, data not shown), but most of these cells were $CD44^{low}$, as expected (data not shown), and there was no increase in tetramer-binding MCMV-specific T cells among the migrated cells (Fig. 6A). All of the other tested chemokines induced significant migration of MCMV-specific T cells (Fig. 6A, 6B). These included chemokines that were expressed at high levels constitutively (CXCL12, CXCL14, CXCL17, and CX3CL1), as well as chemokines induced in the salivary gland by infection (CXCL9, CXCL10, and CCL5) (Fig. 6). These data show that MCMV-specific T cells can migrate in vitro toward several chemokines that are induced by MCMV infection or constitutively expressed in the salivary gland.

Next, we used flow cytometry to explore chemokine receptor expression by OT-I T cells in the spleen and salivary gland 7–9 d after MCMV-OVA infection. Cells were further differentiated by KLRG1 expression, because our previous data showed that most KLRG1-expressing T cells failed to accumulate in the parenchyma of the salivary gland (11). Seven to nine days after MCMV-OVA infection, KLRG1-expressing splenic OT-I T cells were mostly $CX3CR1^+$ $CXCR3^-$, which is consistent with recent studies (71, 72). Additionally, we found that these $KLRG1^+$ cells expressed CXCR6 but mostly lacked CXCR4 (Fig. 7A). In contrast, $KLRG1^-$ splenic OT-I T cells contained subsets expressing or lacking CX3CR1, and a higher frequency of $KLRG1^-$ cells expressed CXCR3, CXCR4, and CXCR6 (Fig. 7A). Of note, these phenotypes were consistent: at 7 mo after MCMV infection, KLRG1 expression on MCMV-specific T cells still correlated with the expression of CX3CR1 and a lack of CXCR3 (data not shown).

Within the parenchyma of the salivary gland, the majority of cells lacked CX3CR1 and KLRG1 (Fig. 7B, left panel). In sharp contrast, T cells found in the vasculature of the salivary gland (i.e., stained by the intravascular Ab) were almost entirely $CX3CR1^+$, and most also expressed KLRG1 (Fig. 7B, right panel). We have had difficulty getting consistent staining of any other chemokine receptors on T cells extracted from the salivary glands. In our hands, CXCR3 has been sensitive to the collagenase used to extract T cells from the salivary gland, and attempts at extracting T cells without collagenase have failed to result in sufficient T cell recovery. Therefore, we measured the expression of chemokine receptors on T cells sorted from the spleen and salivary gland using reverse transcriptase quantitative PCR (RT-qPCR). Naive WT OT-I T cells were transferred into congenic mice and driven to expand with a MCMV-OVA infection. Seven days later, OT-I T cells sorted from the spleen and salivary gland expressed CX3CR1, CCR5, CXCR3, CXCR4, and CXCR6 (Fig. 7C, 7D). In contrast, CCR10 (receptor for CCL28) and CXCR7 (one receptor for CXCL14) were undetectable on spleen- or salivary gland–localized OT-I T cells (data not shown). Interestingly, although salivary gland– and spleen-localized T cells expressed comparable amounts of CXCR3 and CCR5, salivary gland–localized T cells expressed more CXCR4 ($p = 0.016$) and CXCR6 ($p = 0.023$) than spleen-localized T cells. In contrast, spleen-localized T cells expressed much more CX3CR1 than salivary gland–localized T cells ($p < 0.0001$, Fig. 7C, 7D), consistent with our FACS data.

CXCR3 is critical for T cell migration to uninfected salivary glands but is dispensable after MCMV infection

Because MCMV infection induced chemokines that bind CCR5 and CXCR3, we directly tested whether these receptors were critical for the accumulation of MCMV-specific T cells in the salivary gland. To this end, OT-I T cells that expressed or lacked either receptor were mixed with their WT counterparts and cotransferred to congenic B6 recipients. Recipient mice were infected on the following day with MCMV expressing OVA. Two

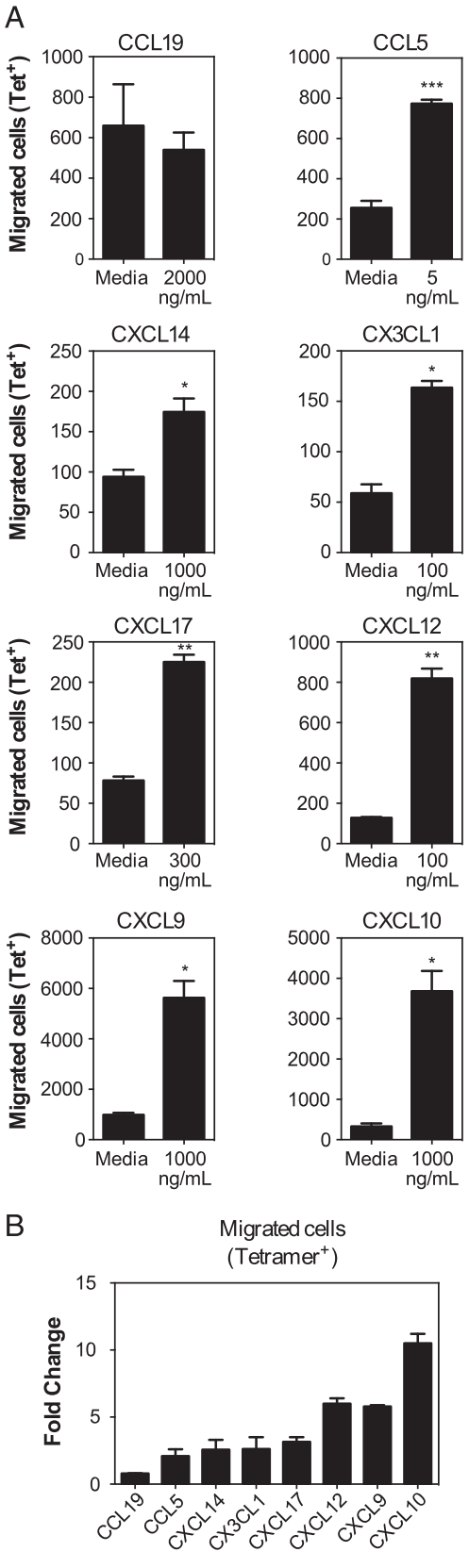

weeks after the infection, there were only small reductions in the numbers of CXCR3-KO or CCR5-KO OT-I T cells in the salivary gland (Fig. 8A, 8C), and these small differences were mirrored in the spleens of the same animals, implying no impairment in the recruitment of T cells lacking CXCR3 (Fig. 8A) or CCR5 (Fig. 8C) receptor. Moreover, there were no differences in the absolute numbers of OT-I T cells that expressed the tissue-resident markers CD69 and CD103 in the gland (Fig. 8B, 8D).

It was possible that CCR5 and CXCR3 played redundant roles in the migration of T cells to the salivary gland during MCMV infection. To address this possibility, WT and CCR5-KO OT-I T cells were activated in vitro and transferred into infected mice, with or without an Ab specific for CXCR3 that has been reported to block CXCR3-dependent cell migration (73, 74). For infection, we used the K181 strain of MCMV lacking OVA, again to avoid the influence of Ag and additional T cell expansion after adoptive transfer. However, donor OT-I T cells still migrated to the salivary gland in all cases, and the absolute number of T cells in the gland was similar in both groups, independently of the CXCR3 blockade (Fig. 8F). There was a subtle difference in the overall number between WT OT-I T cells in the unblocked group and CCR5-KO OT-I T cells in the CXCR3-blocked group, possibly suggesting a combined impact of CXCR3 and CCR5 on T cell migration. However, the effect was subtle, and CXCR3 blockade had an impact in the spleen in all mice. Therefore, it is difficult to distinguish whether this effect was partially due to differences in T cells in circulation (Fig. 8F). There was no impact of CCR5 deficiency, with or without CXCR3 blockade, on T cell migration to lungs or kidneys. Although it is possible that CXCR3 blockade was poorly effective in vivo in infected mice, these data suggest that CCR5 and CXCR3 are not required for T cell accumulation in infected salivary glands.

As a control for these experiments, we transferred in vitro–activated WT OT-I T cells to naive recipients, with or without CXCR3 blockade. Surprisingly, in naive mice, CXCR3 blockade had a striking impact on T cell accumulation in the salivary gland (Fig. 9), resulting in an ~9-fold reduction in the numbers of OT-I T cells that reached the parenchyma (Fig. 9B). Although the blockade had an impact on the numbers of OT-I T cells in the spleen, as in infected mice (Fig. 8F), it was weaker than the impact on the salivary gland in naive mice, and there was no effect on the T cells recovered from the lungs or kidneys (Fig. 9B). These data imply that the CXCR3 blockade was effective in naive mice and suggest that it was having a specific impact on T cell accumulation in the salivary glands of naive mice, despite the absence of an effect in infected mice.

To confirm these surprising results, as well as to determine whether CXCR3 was needed on T cells specifically, CXCR3-KO and WT OT-I T cells were activated in vitro, mixed together, and cotransferred to naive mice. Four days after transfer, the absolute numbers of each OT-I population was assessed, and the ratio of KO/WT cells was calculated within the parenchyma and the circulation. In line with our blocking Ab data, accumulation of CXCR3-KO OT-I T cells in the salivary gland was markedly impaired in two separate experiments (Fig. 9D, 9E). Together, these data strongly imply that T cell migration to, as well as accumulation in, uninfected salivary glands critically depends on CXCR3.

FIGURE 6. MCMV-specific $CD8^+$ T cells migrate toward multiple chemokines. Mice were sacrificed 7 d after i.p. MCMV infection. $CD8^+$ T cells were enriched and used to perform Transwell migration assays with multiple chemokines. Assays were performed with replicates, and media control was included in each assay to account for plate-to-plate variation. (**A**) Absolute numbers of MCMV-specific T cells (M45 $Tetramer^+$ plus M38 $Tetramer^+$) that migrated toward the indicated chemokine in comparison with control wells containing media and cells, but no chemokine. Data are from a single experiment performed in triplicate or quadruplicate and are representative of two to five experiments per chemokine. (**B**) Fold change in migration in comparison with media. Pooled data from two to four independent experiments indicating the fold change of migration of MCMV-specific cells (M45 $Tetramer^+$ plus M38 $Tetramer^+$) in response to the indicated chemokines at the concentrations shown in (A). $*p < 0.05$, $**p < 0.01$, $***p < 0.001$, paired t test.

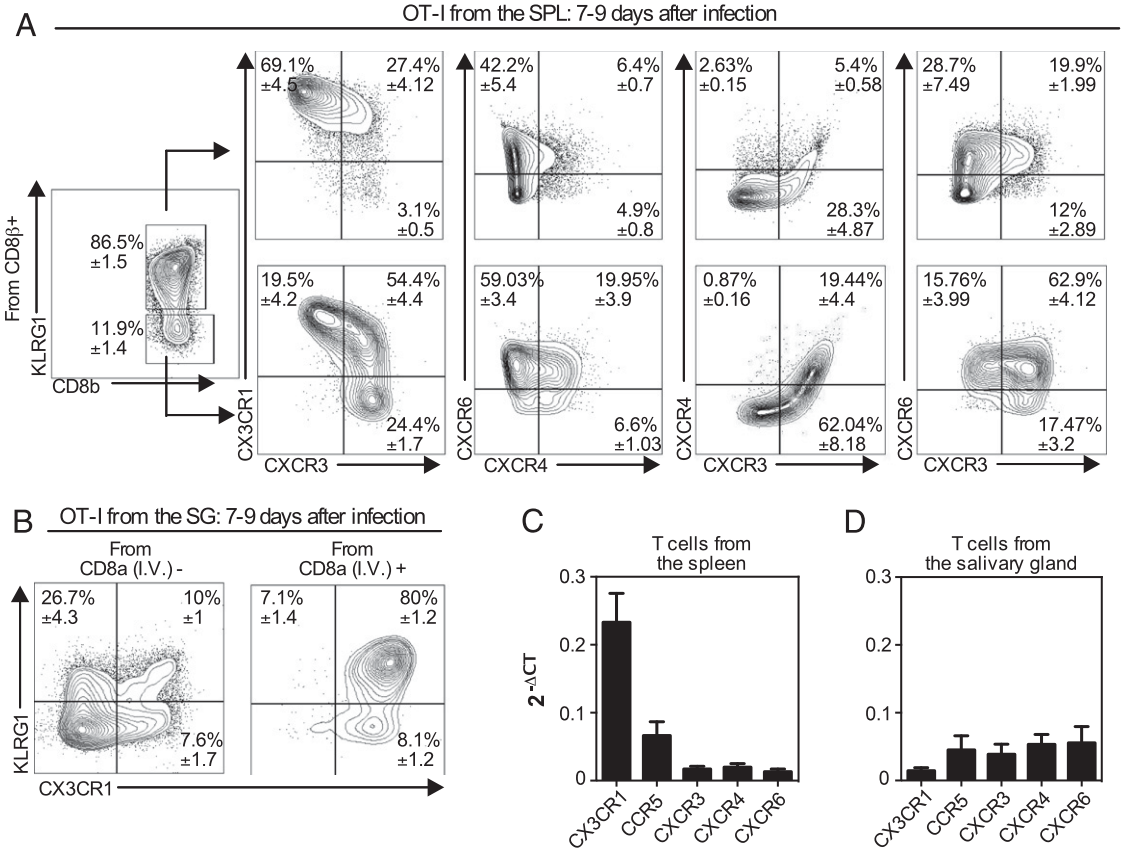

FIGURE 7. Most $CD8^+$ T cells in the parenchyma of the salivary gland lack KLRG1 and CX3CR1 but express multiple other chemokine receptors. Naive OT-I T cells (2×10^3) were transferred to naive B6 mice that were infected i.p. 1 d later with MCMV expressing OVA. Mice were sacrificed 7 or 9 d postinfection. (**A**) Chemokine receptor expression within the $KLRG1^+$ and $KLRG1^-$ subsets of OT-I T cells in the spleen. (**B**) KLRG1 and CX3CR1 expression of OT-I T cells from the vasculature ($I.V.^+$) and parenchyma ($I.V.^-$) portions of the salivary gland. Data show concatenated FACS plots from one representative experiment at day 9 ($n = 3$), with mean ± SEM values in each quadrant derived from all experiments (total $n = 8$). (**C** and **D**) Naive OT-I T cells were transferred as in (A) and sorted from the spleen (C) and the salivary gland (D) 7 d postinfection with MCMV expressing OVA. Chemokine receptor expression was assessed on sorted T cells by RT-qPCR. Data were combined from two to five independent RT-qPCR assays per sample, with cDNA from OT-I T cells sorted from two to three independent mice. Error bars represent SEM.

CXCL9 is expressed in the salivary gland at steady-state, even in the absence of IFN-γ

Because the ligands for CXCR3 (CXCL9 and CXCL10 in B6 mice) are strongly induced by IFN-γ and upregulated by MCMV infection (Fig. 5), we wished to confirm that these ligands were present in naive mice and test whether IFN-γ was required for T cell migration to the salivary gland. The chemokine CXCL9 was readily detectable by ELISA and RT-qPCR in the salivary glands of naive B6 and was also evident in IFN-γ–KO mice (Fig. 9F, 9G). In addition, when in vitro–activated OT-I T cells were transferred to naive IFN-γ–KO or B6 mice, they reached the salivary gland in similar numbers (Fig. 9H). Thus, CXCL9 is available for T cell recruitment to uninfected salivary glands, with or without infection or IFN-γ. Collectively, these data suggest that the integrin $\alpha_4\beta_1$ and the chemokine receptor CXCR3 play critical roles in the recruitment of T cells to uninfected or noninflamed salivary glands but that CXCR3 is redundant during inflammation induced by MCMV infection.

Discussion

The salivary gland is an important site of viral infection for transmission to new hosts. Indeed, all betaherpesviruses and gammaherpesviruses infect the salivary gland and are shed into saliva. Moreover, herpesviruses like CMV establish latency in the salivary gland and reactivate readily in this site during periods of immune suppression, particularly when $CD8^+$ T cells have been depleted (9). Therefore, it is important to understand the mechanisms that promote and establish $CD8^+$ T cell residency in the salivary gland.

Recent studies have shown that salivary gland–localized T cells can become T_{RM} that reside near or within the epithelial layer (10, 11). Interestingly, the mechanisms governing T_{RM} formation and maintenance differ in different tissues (75). Although TGF-β is described as critical for promoting CD103-expressing T_{RM} in most tissues tested to date, including the salivary gland, a role for Ag and inflammation is more variable (10, 11, 15, 21, 25, 76). Ag seems to be required for the formation of $CD103^+$ T_{RM} in the CNS and lungs (19, 20, 77). In the skin, the efficiency of T cell recruitment is poor without local inflammation, and Ag improves T_{RM} maintenance, as well as the selection of T_{RM} specificities (16, 24). In contrast, T_{RM} can form in the small intestine independently of Ag, infection, or commensal microbiota. In fact, Ag in the small intestine may reduce expression of CD103 on T cells that reach this tissue (28). Remarkably, like the small intestine, the salivary gland seems capable of recruiting activated T cells in the absence of a specific infection or inflammation (10–12). In fact, our data show that naive uninfected salivary glands and those with an active MCMV infection were equally capable of recruiting activated T cells over a period of 31 d (Fig. 3). These data suggest that the salivary gland and small intestine may represent a set of tissues that is continuously surveyed by activated T cells and is capable of inducing their retention through constitutive TGF-β

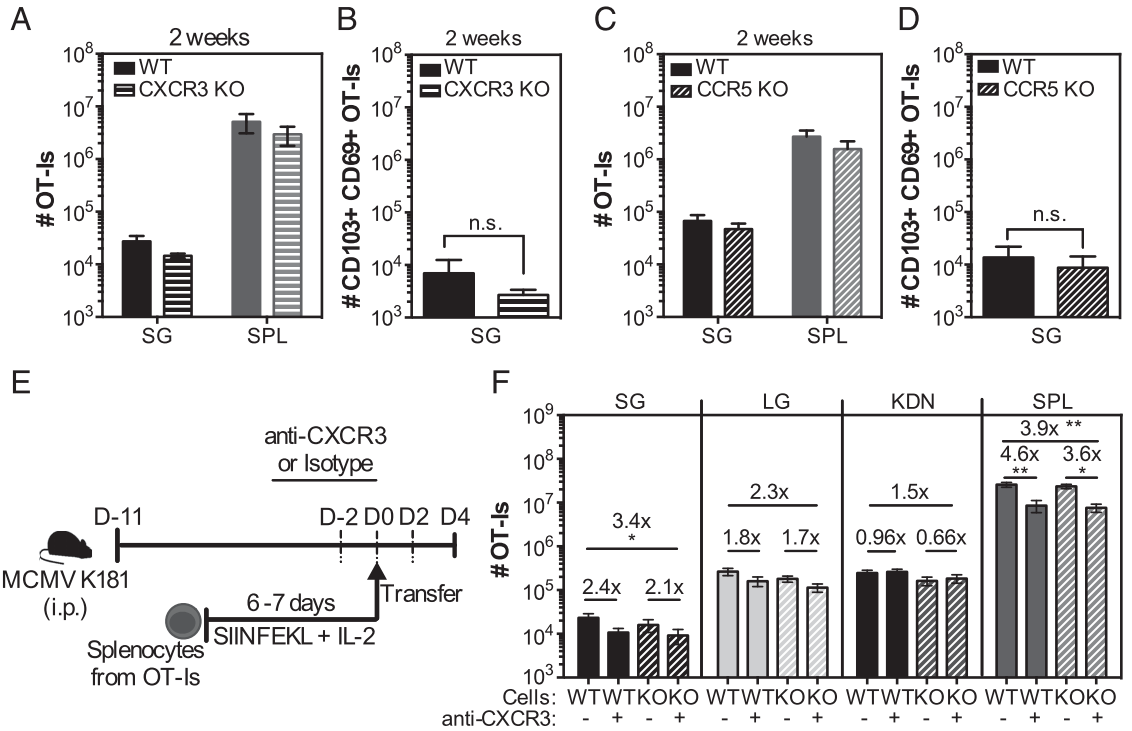

FIGURE 8. Lack of CXCR3 or CCR5 does not impact the accumulation of $CD8^+$ T cells in the salivary gland after MCMV infection. (**A** and **C**) WT OT-I T cells and OT-I T cells that lacked the chemokine receptor CXCR3 or CCR5 were mixed (1×10^3 of each) and cotransferred to naive B6 mice that were subsequently infected with MCMV-OVA. Overall numbers of CXCR3-KO (A) or CCR5-KO (C) OT-I T cells versus WT OT-I T cells from the spleen (SPL) and the parenchyma of the salivary gland (SG) 14 d postinfection. (**B** and **D**) Absolute numbers of $CD103^+$ $CD69^+$ OT-I T cells from the SG. Data are combined from two independent experiments for each KO/WT pair ($n = 7$ for WT/CXCR3 experiments, $n = 5$ for WT/CCR5 experiments). (**E**) Experimental design of the OT-I adoptive transfer for (**F**). WT and CCR5-KO OT-I T cells were activated in vitro, and 4×10^6 of each were mixed. Mixed cells were treated with anti-CXCR3 Ab or an isotype control and cotransferred to MCMV-infected mice that were treated with anti-CXCR3 or an isotype control Ab via i.p. injection every other day starting 2 d before the adoptive transfer. (F) Absolute numbers of WT (solid bars) or CCR5-KO (striped bars) OT-I T cells in the parenchyma of the salivary gland (SG), lungs (LG), and kidneys (KDN), as well as from the overall $CD8\beta^+$ T cells from the spleen (SPL) of CXCR3-blocked (+) or isotype control–treated (-) mice. Data are from two independent experiments ($n = 7$ for the isotype-treated group, $n = 8$ for the CXCR3-treated group). Error bars represent that SEM. The statistical significance was measured by an unpaired t test after $\log_{10}$ conversion of the absolute numbers (A–D) and by one-way ANOVA (F). $^*p < 0.05$, $^{**}p < 0.01$. n.s., not significant.

expression. T cell recruitment to naive and infected salivary glands depended on the α_4 integrin (Fig. 4), whereas recruitment to naive salivary glands depended on the chemokine receptor CXCR3 (Fig. 9). These results imply that sufficient levels of VCAM-1 and CXCR3 ligands are expressed at steady-state in the salivary gland for T cell recruitment. Indeed, CXCL9 was detectable in the salivary glands of naive B6 mice, and its expression was not dependent on IFN-γ (Fig. 9). These data establish a mechanism for the recruitment of activated T cells to the salivary gland, regardless of infection.

Given that CXCL9 is classically thought of as an IFN-γ–induced chemokine, it is interesting that it was constitutively expressed in the salivary gland. It is possible that animal colony conditions or husbandry practices within our animal colony contribute to the constitutive expression of CXCL9 that we observed (Fig. 9) and the constitutive ability of naive salivary glands to recruit T cells (Fig. 3). However, the recruitment of T cells to the salivary gland in naive mice has been demonstrated in two other laboratories (10, 12), suggesting that our results cannot be explained by housing conditions in the Thomas Jefferson University animal facility. It must be noted that the salivary gland ducts are open to the oral cavity and, therefore, are likely to be colonized by the oral microbiome. Thus, it is possible that CXCL9 expression is a direct response to oral microbiota. Interestingly, several chemokines, including CXCL9, CXCL10, and CXCL11, can have antimicrobial functions (78–80). Therefore, it is possible that T cell recruitment is secondary to the antimicrobial role of chemokines in the salivary gland and perhaps other digestive tissues. It will be fascinating in future work to determine whether CXCL9 levels, as well as the steady-state recruitment of activated T cells to the salivary gland, are controlled by the oral microbiome.

Although CXCR3 appears to play a crucial role in the recruitment of T cells to naive salivary glands, it is important to note that our experiments did not test whether CXCL9 and CXCL10 were required to recruit activated T cells to the naive or infected salivary glands. Indeed, it is possible that CXCR3 was being activated by alternative ligands in naive mice or that CXCL9 and CXCL10 could use alternative chemokine receptors in infected mice. Moreover, heterodimerization of chemokines, as well as heterodimerization of receptors, has been described and can increase the breadth of potential ligand/receptor interactions (81, 82). Therefore, extensive future work will be needed to tease apart the specific ligand/receptor interactions involved in T cell recruitment in different settings.

Although infected salivary glands recruited activated OT-I T cells more rapidly, we observed a plateau in recruitment (Fig. 3). It is possible that the ultimate numbers of T_{RM} that accumulated in the salivary gland may have depended on the potential of the T cells induced by in vitro activation. In our hands, a subset of in vitro–activated OT-I T cells expressed CXCR3, CXCR4, and/or CXCR6, and the population, as a whole, almost completely lacked CX3CR1 (data not shown), much like our

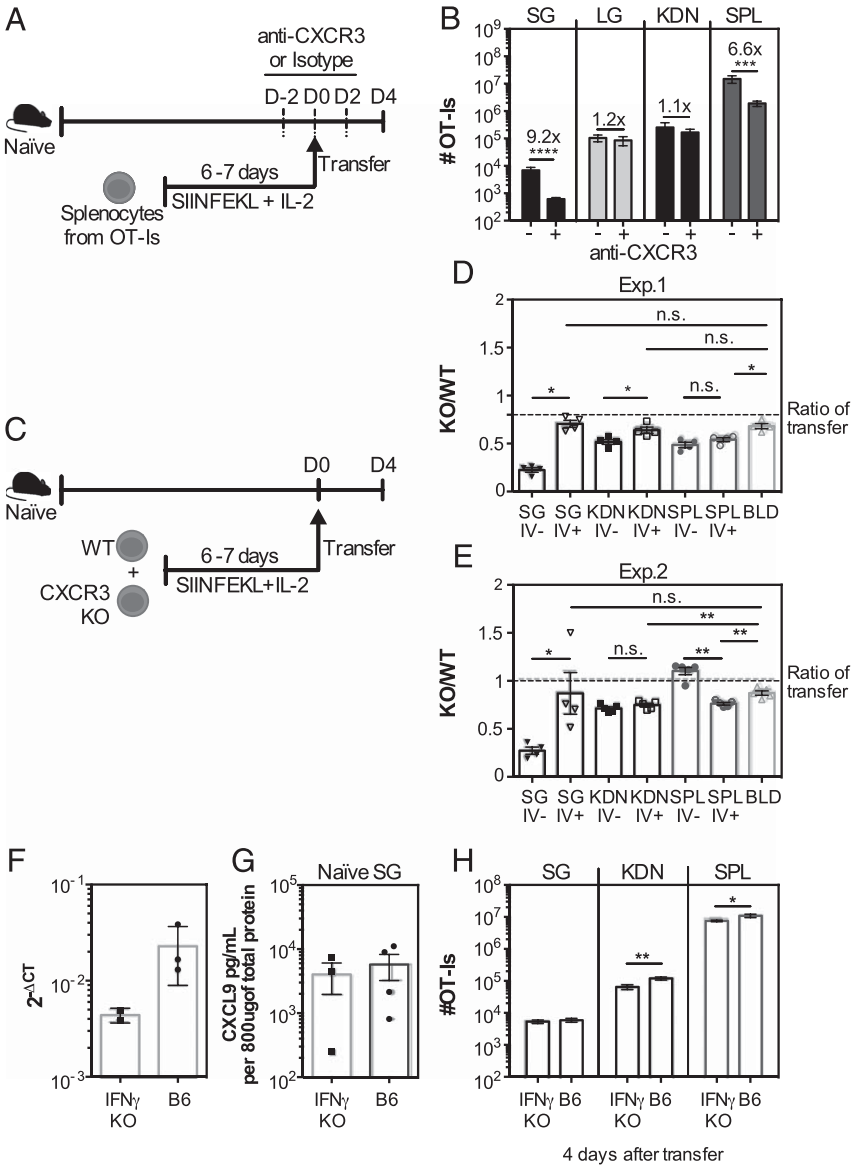

FIGURE 9. CXCR3 blockade reduces the recruitment of $CD8^+$ T cells to salivary glands in uninfected mice independently of IFN-γ. (**A**) WT OT-I T cells were activated in vitro and treated with anti-CXCR3 Ab or isotype control, and 4×10^6 cells were transferred to naive mice. The recipients were also treated with anti-CXCR3 Ab or isotype control every other day, starting 2 d before transfer until sacrifice. (**B**) Absolute numbers of OT-I T cells that reached the parenchyma of the salivary gland (SG), lungs (LG), and kidneys (KDN), as well as from the $CD8\beta^+$ population of the spleen (SPL). Data are from two independent experiments ($n = 7$ for the isotype-treated group, $n = 8$ for the group treated with anti-CXCR3). (**C**) Experimental design for (**D**) and (**E**). WT and CXCR3-KO OT-I T cells were activated in vitro, and 4×10^6 of each were mixed and cotransferred to naive mice. (D and E) Ratio of KO/WT OT-I T cells in the vasculature ($I.V.^-$) and parenchyma ($I.V.^+$) of the SG, KDN, and SPL, as well as from the overall $CD8\beta^+$ cells in the blood. Two independent experiments are shown [$n = 4$ in (D), $n = 5$ in (E)]. The dashed lines represent the ratio of KO/WT cells in the transferred pool (as assessed by FACS on the day of transfer). The levels of CXCL9 in the SG of naive B6 and IFN-γ–KO mice were determined by RT-qPCR (**F**) and ELISA (**G**). Data are from one experiment [$n = 2$ or 3 (F), $n = 3$ or 4 (G)]. (**H**) WT OT-I T cells were activated in vitro, and 4×10^6 T cells were transferred to naive B6 or IFN-γ–KO mice [similarly to (A and B)]. Four days after transfer, the organs were collected; the overall numbers of OT-I T cells in the SG, KDN, and SPL are shown. Data are pooled from two independent experiments ($n = 6$ B6 mice, $n = 7$ IFN-γ–KO mice). Error bars represent the SEM. For (A) and (H), statistical significance was measured by an unpaired t test after log10 conversion of the absolute numbers. For (D) and (E), the ratio of KO to WT cells was compared between the blood, the IV+ and the IV− fractions of each organ using a nonparametric Mann–Whitney test. $*p < 0.05$, $**p < 0.01$, $***p < 0.001$, $****p < 0.0001$. n.s., not significant.

MCMV-specific T cells in the salivary gland (Fig. 7). However, we cannot exclude the possibility that only a subset of activated OT-I T cells was capable of migrating to the salivary gland and becoming T_{RM}, which could simulate a plateau in OT-I T_{RM} numbers in the salivary gland over time. However, if such a limit in cell numbers existed, it was unlikely to be caused by competition for space or environmental cues in the salivary gland. New OT-I or VACV-specific T_{RM} were able to form in the salivary glands of mice previously infected with MCMV (Fig. 2, data not shown), despite the fact that infected salivary glands contained 20–30-fold more T cells than naive salivary glands (data not shown). Together, these experiments suggest that the salivary gland can accommodate more T_{RM} than were induced in our experimental systems. Nevertheless, it is possible that pre-existing T_{RM} in the salivary gland would be reduced over time in animals exposed to repeated infections. Thus, it will be exciting to learn how salivary gland–localized T_{RM} populations would evolve over time in response to multiple different infections.

Our data showed that most KLRG1-expressing MCMV-specific T cells upregulated CX3CR1 but lost CXCR3 expression and failed to migrate into the salivary gland, even during MCMV infection (Fig. 7). However, CXCR3 deficiency did not preclude MCMV-specific T cells from the salivary gland during infection (Fig. 8). Thus, presumably the loss of CXCR3 alone was not responsible for the inability of these T cells to migrate into the salivary gland. Moreover, a lack of the α_4 integrin cannot explain the failure of these cells to enter the salivary gland, because we have seen comparable expression of α_4 integrin on KLRG1$^+$ and KLRG$^-$ MCMV-specific T cells (data not shown). These results were surprising to us, but also broadly consistent with research by Pircher and colleagues (32) that suggested that CXCR3 was dispensable for CD8$^+$ T cell migration to the salivary gland after lymphocytic choriomeningitis virus strain WE (LCMV-WE) infection. LCMV-WE is reported to not infect the salivary gland directly (12), and it is unclear whether CXCR3 ligands in the salivary gland are increased by LCMV-WE infection. Regardless, it is certain that other changes induced by infection will contribute to the efficiency and speed of T cell recruitment. Indeed, LCMV-WE infection was associated with an increase in VCAM-1 on the salivary gland vascular endothelium that likely facilitated the recruitment of T cells. Thus, it is possible that MCMV infection reduced the burden on CXCR3 by increasing additional molecules that are involved in the recruitment of T cells. Another possible explanation is that MCMV infection induced an array of chemokines that could redundantly recruit T cells. We tested whether CCR5 and CXCR3 were acting together to recruit T cells by blocking CXCR3 on CCR5-KO T cells. However, these results should be interpreted cautiously. Although CXCR3 blockade reduced T cell recruitment to the salivary gland in naive mice, it is unclear whether the Ab was fully able to block the CXCR3 receptor in infected mice, which likely have many more CXCR3-expressing cells. Future work will need to explore the specific mechanisms used by T cells to enter the salivary gland during acute MCMV infection.

In conclusion, our data show that the salivary gland is able to constitutively recruit CD8$^+$ T cells in a α_4 integrin– and CXCR3-dependent manner and subsequently induce and sustain T_{RM} populations in the absence of infection, Ag, or inflammation. Thus, it is plausible to think that the T_{RM} populations in the salivary gland, and perhaps other tissues in the digestive tract, will retain a record of previous infections and their specificities, regardless of whether those infections were related to the salivary gland. Moreover, the fact that CXCR3 was critical for recruitment of T cells to naive salivary glands should be useful for guiding the future development of vaccines that aim to establish or boost the mucosal immune responses in the salivary gland.

Acknowledgments

We thank Gudrun F. Debes for technical support with chemotaxis assays and guidance about chemokines and chemokine receptors.

Disclosures

The authors have no financial conflicts of interest.

References

1. Cannon, M. J., J. D. Stowell, R. Clark, P. R. Dollard, D. Johnson, K. Mask, C. Stover, K. Wu, M. Amin, W. Hendley, et al. 2014. Repeated measures study of weekly and daily cytomegalovirus shedding patterns in saliva and urine of healthy cytomegalovirus-seropositive children. *BMC Infect. Dis.* 14: 569.
2. Harnett, G. B., T. J. Farr, G. R. Pietroboni, and M. R. Bucens. 1990. Frequent shedding of human herpesvirus 6 in saliva. *J. Med. Virol.* 30: 128–130.
3. Miller, C. S., J. R. Berger, Y. Mootoor, S. A. Avdiushko, H. Zhu, and R. J. Kryscio. 2006. High prevalence of multiple human herpesviruses in saliva from human immunodeficiency virus-infected persons in the era of highly active antiretroviral therapy. *J. Clin. Microbiol.* 44: 2409–2415.
4. Reddehase, M. J., M. Balthesen, M. Rapp, S. Jonjić, I. Pavić, and U. H. Koszinowski. 1994. The conditions of primary infection define the load of latent viral genome in organs and the risk of recurrent cytomegalovirus disease. *J. Exp. Med.* 179: 185–193.
5. Jonjić, S., W. Mutter, F. Weiland, M. J. Reddehase, and U. H. Koszinowski. 1989. Site-restricted persistent cytomegalovirus infection after selective long-term depletion of CD4+ T lymphocytes. *J. Exp. Med.* 169: 1199–1212.
6. Crough, T., and R. Khanna. 2009. Immunobiology of human cytomegalovirus: from bench to bedside. *Clin. Microbiol. Rev.* 22: 76–98.
7. Henson, D., and A. J. Strano. 1972. Mouse cytomegalovirus. Necrosis of infected and morphologically normal submaxillary gland acinar cells during termination of chronic infection. *Am. J. Pathol.* 68: 183–202.
8. Krmpotic, A., I. Bubic, B. Polic, P. Lucin, and S. Jonjic. 2003. Pathogenesis of murine cytomegalovirus infection. *Microbes Infect.* 5: 1263–1277.
9. Polić, B., H. Hengel, A. Krmpotić, J. Trgovcich, I. Pavić, P. Luccaronin, S. Jonjić, and U. H. Koszinowski. 1998. Hierarchical and redundant lymphocyte subset control precludes cytomegalovirus replication during latent infection. *J. Exp. Med.* 188: 1047–1054.
10. Thom, J. T., T. C. Weber, S. M. Walton, N. Torti, and A. Oxenius. 2015. The salivary gland acts as a sink for tissue-resident memory CD8(+) T cells, facilitating protection from local cytomegalovirus infection. *Cell Reports* 13: 1125–1136.
11. Smith, C. J., S. Caldeira-Dantas, H. Turula, and C. M. Snyder. 2015. Murine CMV infection induces the continuous production of mucosal resident T cells. *Cell Reports* 13: 1137–1148.
12. Hofmann, M., and H. Pircher. 2011. E-cadherin promotes accumulation of a unique memory CD8 T-cell population in murine salivary glands. *Proc. Natl. Acad. Sci. USA* 108: 16741–16746.
13. Schenkel, J. M., and D. Masopust. 2014. Tissue-resident memory T cells. *Immunity* 41: 886–897.
14. Mueller, S. N., and L. K. Mackay. 2016. Tissue-resident memory T cells: local specialists in immune defence. *Nat. Rev. Immunol.* 16: 79–89.
15. Mackay, L. K., A. Rahimpour, J. Z. Ma, N. Collins, A. T. Stock, M.-L. Hafon, J. Vega-Ramos, P. Lauzurica, S. N. Mueller, T. Stefanovic, et al. 2013. The developmental pathway for CD103(+)CD8+ tissue-resident memory T cells of skin. *Nat. Immunol.* 14: 1294–1301.
16. Khan, T. N., J. L. Mooster, A. M. Kilgore, J. F. Osborn, and J. C. Nolz. 2016. Local antigen in nonlymphoid tissue promotes resident memory CD8+ T cell formation during viral infection. *J. Exp. Med.* 213: 951–966.
17. Nakanishi, Y., B. Lu, C. Gerard, and A. Iwasaki. 2009. CD8(+) T lymphocyte mobilization to virus-infected tissue requires CD4(+) T-cell help. *Nature* 462: 510–513.
18. Hogan, R. J., E. J. Usherwood, W. Zhong, A. A. Roberts, R. W. Dutton, A. G. Harmsen, and D. L. Woodland. 2001. Activated antigen-specific CD8+ T cells persist in the lungs following recovery from respiratory virus infections. *J. Immunol.* 166: 1813–1822.
19. Morabito, K. M., T. R. Ruckwardt, A. J. Redwood, S. M. Moin, D. A. Price, and B. S. Graham. 2017. Intranasal administration of RSV antigen-expressing MCMV elicits robust tissue-resident effector and effector memory CD8+ T cells in the lung. *Mucosal Immunol.* 10: 545–554.
20. Wakim, L. M., A. Woodward-Davis, and M. J. Bevan. 2010. Memory T cells persisting within the brain after local infection show functional adaptations to their tissue of residence. *Proc. Natl. Acad. Sci. USA* 107: 17872–17879.
21. Lee, Y.-T., J. E. Suarez-Ramirez, T. Wu, J. M. Redman, K. Bouchard, G. A. Hadley, and L. S. Cauley. 2011. Environmental and antigen receptor-derived signals support sustained surveillance of the lungs by pathogen-specific cytotoxic T lymphocytes. *J. Virol.* 85: 4085–4094.
22. Mackay, L. K., A. T. Stock, J. Z. Ma, C. M. Jones, S. J. Kent, S. N. Mueller, W. R. Heath, F. R. Carbone, and T. Gebhardt. 2012. Long-lived epithelial immunity by tissue-resident memory T (TRM) cells in the absence of persisting local antigen presentation. *Proc. Natl. Acad. Sci. USA* 109: 7037–7042.
23. Davies, B., J. E. Prier, C. M. Jones, T. Gebhardt, F. R. Carbone, and L. K. Mackay. 2017. Cutting edge: tissue-resident memory T cells generated by multiple immunizations or localized deposition provide enhanced immunity. *J. Immunol.* 198: 2233–2237.
24. Muschaweckh, A., V. R. Buchholz, A. Fellenzer, C. Hessel, P.-A. König, S. Tao, R. Tao, M. Heikenwälder, D. H. Busch, T. Korn, et al. 2016. Antigen-dependent competition shapes the local repertoire of tissue-resident memory CD8 + T cells. *J. Exp. Med.* 213: 3075–3086.
25. Jiang, X., R. A. Clark, L. Liu, A. J. Wagers, R. C. Fuhlbrigge, and T. S. Kupper. 2012. Skin infection generates non-migratory memory CD8+ T(RM) cells providing global skin immunity. *Nature* 483: 227–231.
26. Wu, T., Y. Hu, Y.-T. Lee, K. R. Bouchard, A. Benechet, K. Khanna, and L. S. Cauley. 2014. Lung-resident memory CD8 T cells (TRM) are indispensable for optimal cross-protection against pulmonary virus infection. *J. Leukoc. Biol.* 95: 215–224.
27. Venturi, V., K. Nzingha, T. G. Amos, W. C. Charles, I. Dekhtiarenko, L. Cicin-Sain, M. P. Davenport, and B. D. Rudd. 2016. The neonatal CD8+ T cell repertoire rapidly diversifies during persistent viral infection. *J. Immunol.* 196: 1604–1616.
28. Casey, K. A., K. A. Fraser, J. M. Schenkel, A. Moran, M. C. Abt, L. K. Beura, P. J. Lucas, D. Artis, E. J. Wherry, K. Hogquist, et al. 2012. Antigen-independent differentiation and maintenance of effector-like resident memory T cells in tissues. *J. Immunol.* 188: 4866–4875.

29. Sato, T., H. Thorlacius, B. Johnston, T. L. Staton, W. Xiang, D. R. Littman, and E. C. Butcher. 2005. Role for CXCR6 in recruitment of activated CD8+ lymphocytes to inflamed liver. *J. Immunol.* 174: 277–283.
30. Hamann, A., D. P. Andrew, D. Jablonski-Westrich, B. Holzmann, and E. C. Butcher. 1994. Role of alpha 4-integrins in lymphocyte homing to mucosal tissues in vivo. *J. Immunol.* 152: 3282–3293.
31. Campbell, D. J., and E. C. Butcher. 2002. Intestinal attraction: CCL25 functions in effector lymphocyte recruitment to the small intestine. *J. Clin. Invest.* 110: 1079–1081.
32. Woyciechowski, S., M. Hofmann, and H. Pircher. 2017. α4 β1 integrin promotes accumulation of tissue-resident memory CD8+ T cells in salivary glands. *Eur. J. Immunol.* 47: 244–250.
33. Groom, J. R., and A. D. Luster. 2011. CXCR3 in T cell function. *Exp. Cell Res.* 317: 620–631.
34. Turula, H., C. J. Smith, F. Grey, K. A. Zurbach, and C. M. Snyder. 2013. Competition between T cells maintains clonal dominance during memory inflation induced by MCMV. *Eur. J. Immunol.* 43: 1252–1263.
35. Cunningham, P. T., M. L. Lloyd, N. L. Harvey, E. Williams, C. M. Hardy, A. J. Redwood, M. A. Lawson, and G. R. Shellam. 2010. Promoter control over foreign antigen expression in a murine cytomegalovirus vaccine vector. *Vaccine* 29: 141–151.
36. Farrington, L. A., T. A. Smith, F. Grey, A. B. Hill, and C. M. Snyder. 2013. Competition for antigen at the level of the APC is a major determinant of immunodominance during memory inflation in murine cytomegalovirus infection. *J. Immunol.* 190: 3410–3416.
37. Zurbach, K. A., T. Moghbeli, and C. M. Snyder. 2014. Resolving the titer of murine cytomegalovirus by plaque assay using the M2-10B4 cell line and a low viscosity overlay. *Virol. J.* 11: 71.
38. Snyder, C. M., K. S. Cho, E. L. Bonnett, J. E. Allan, and A. B. Hill. 2011. Sustained CD8+ T cell memory inflation after infection with a single-cycle cytomegalovirus. *PLoS Pathog.* 7: e1002295.
39. Anderson, K. G., H. Sung, C. N. Skon, L. Lefrancois, A. Deisinger, V. Vezys, and D. Masopust. 2012. Cutting edge: intravascular staining redefines lung CD8 T cell responses. *J. Immunol.* 189: 2702–2706.
40. Smith, C. J., H. Turula, and C. M. Snyder. 2014. Systemic hematogenous maintenance of memory inflation by MCMV infection. *PLoS Pathog.* 10: e1004233.
41. Snyder, C. M., K. S. Cho, E. L. Bonnett, S. van Dommelen, G. R. Shellam, and A. B. Hill. 2008. Memory inflation during chronic viral infection is maintained by continuous production of short-lived, functional T cells. *Immunity* 29: 650–659.
42. Liao, Y., G. K. Smyth, and W. Shi. 2014. featureCounts: an efficient general purpose program for assigning sequence reads to genomic features. *Bioinformatics* 30: 923–930.
43. Love, M. I., W. Huber, and S. Anders. 2014. Moderated estimation of fold change and dispersion for RNA-seq data with DESeq2. *Genome Biol.* 15: 550.
44. Subramanian, A., P. Tamayo, V. K. Mootha, S. Mukherjee, B. L. Ebert, M. A. Gillette, A. Paulovich, S. L. Pomeroy, T. R. Golub, E. S. Lander, and J. P. Mesirov. 2005. Gene set enrichment analysis: a knowledge-based approach for interpreting genome-wide expression profiles. *Proc. Natl. Acad. Sci. USA* 102: 15545–15550.
45. Gallichan, W. S., and K. L. Rosenthal. 1996. Long-lived cytotoxic T lymphocyte memory in mucosal tissues after mucosal but not systemic immunization. *J. Exp. Med.* 184: 1879–1890.
46. Takamura, S., A. D. Roberts, D. M. Jelley-Gibbs, S. T. Wittmer, J. E. Kohlmeier, and D. L. Woodland. 2010. The route of priming influences the ability of respiratory virus-specific memory CD8+ T cells to be activated by residual antigen. *J. Exp. Med.* 207: 1153–1160.
47. Sheridan, B. S., Q. M. Pham, Y.-T. Lee, L. S. Cauley, L. Puddington, and L. Lefrançois. 2014. Oral infection drives a distinct population of intestinal resident memory CD8(+) T cells with enhanced protective function. *Immunity* 40: 747–757.
48. Oduro, J. D., A. Redeker, N. A. Lemmermann, L. Ebermann, T. F. Marandu, I. Dekhtiarenko, J. K. Holzki, D. H. Busch, R. Arens, and L. Čičin-Šain. 2016. Murine cytomegalovirus (CMV) infection via the intranasal route offers a robust model of immunity upon mucosal CMV infection. *J. Gen. Virol.* 97: 185–195.
49. Salmi, M., and S. Jalkanen. 2005. Lymphocyte homing to the gut: attraction, adhesion, and commitment. *Immunol. Rev.* 206: 100–113.
50. Iwata, M., A. Hirakiyama, Y. Eshima, H. Kagechika, C. Kato, and S. Y. Song. 2004. Retinoic acid imprints gut-homing specificity on T cells. *Immunity* 21: 527–538.
51. Walch, J. M., Q. Zeng, Q. Li, M. H. Oberbarnscheidt, R. A. Hoffman, A. L. Williams, D. M. Rothstein, W. D. Shlomchik, J. V. Kim, G. Camirand, and F. G. Lakkis. 2013. Cognate antigen directs CD8+ T cell migration to vascularized transplants. *J. Clin. Invest.* 123: 2663–2671.
52. Komai-Koma, M., J. A. Gracie, X. Q. Wei, D. Xu, N. Thomson, I. B. McInnes, and F. Y. Liew. 2003. Chemoattraction of human T cells by IL-18. *J. Immunol.* 170: 1084–1090.
53. Katakai, T., T. Hara, M. Sugai, H. Gonda, Y. Nambu, E. Matsuda, Y. Agata, and A. Shimizu. 2002. Chemokine-independent preference for T-helper-1 cells in transendothelial migration. *J. Biol. Chem.* 277: 50948–50958.
54. Mangmool, S., and H. Kurose. 2011. G(i/o) protein-dependent and -independent actions of Pertussis Toxin (PTX). *Toxins (Basel)* 3: 884–899.
55. Spangrude, G. J., B. A. Braaten, and R. A. Daynes. 1984. Molecular mechanisms of lymphocyte extravasation. I. Studies of two selective inhibitors of lymphocyte recirculation. *J. Immunol.* 132: 354–362.
56. Cyster, J. G., and C. C. Goodnow. 1995. Pertussis toxin inhibits migration of B and T lymphocytes into splenic white pulp cords. *J. Exp. Med.* 182: 581–586.
57. Kohlmeier, J. E., S. C. Miller, J. Smith, B. Lu, C. Gerard, T. Cookenham, A. D. Roberts, and D. L. Woodland. 2008. The chemokine receptor CCR5 plays a key role in the early memory CD8+ T cell response to respiratory virus infections. *Immunity* 29: 101–113.
58. Crispe, I. N. 2012. Migration of lymphocytes into hepatic sinusoids. *J. Hepatol.* 57: 218–220.
59. Galkina, E., J. Thatte, V. Dabak, M. B. Williams, K. Ley, and T. J. Braciale. 2005. Preferential migration of effector CD8+ T cells into the interstitium of the normal lung. *J. Clin. Invest.* 115: 3473–3483.
60. Bardina, S. V., D. Michlmayr, K. W. Hoffman, C. J. Obara, J. Sum, I. F. Charo, W. Lu, A. G. Pletnev, and J. K. Lim. 2015. Differential roles of chemokines CCL2 and CCL7 in monocytosis and leukocyte migration during West Nile virus infection. *J. Immunol.* 195: 4306–4318.
61. Islam, S. A., D. S. Chang, R. A. Colvin, M. H. Byrne, M. L. McCully, B. Moser, S. A. Lira, I. F. Charo, and A. D. Luster. 2011. Mouse CCL8, a CCR8 agonist, promotes atopic dermatitis by recruiting IL-5+ T(H)2 cells. *Nat. Immunol.* 12: 167–177.
62. Loetscher, P., M. Seitz, I. Clark-Lewis, M. Baggiolini, and B. Moser. 1994. Monocyte chemotactic proteins MCP-1, MCP-2, and MCP-3 are major attractants for human CD4+ and CD8+ T lymphocytes. *FASEB J.* 8: 1055–1060.
63. Olive, A. J., D. C. Gondek, and M. N. Starnbach. 2011. CXCR3 and CCR5 are both required for T cell-mediated protection against *C. trachomatis* infection in the murine genital mucosa. *Mucosal Immunol.* 4: 208–216.
64. Hickman, H. D., G. V. Reynoso, B. F. Ngudiankama, S. S. Cush, J. Gibbs, J. R. Bennink, and J. W. Yewdell. 2015. CXCR3 chemokine receptor enables local CD8(+) T cell migration for the destruction of virus-infected cells. *Immunity* 42: 524–537.
65. Wang, W., H. Soto, E. R. Oldham, M. E. Buchanan, B. Homey, D. Catron, N. Jenkins, N. G. Copeland, D. J. Gilbert, N. Nguyen, et al. 2000. Identification of a novel chemokine (CCL28), which binds CCR10 (GPR2). *J. Biol. Chem.* 275: 22313–22323.
66. Kitchen, S. G., S. LaForge, V. P. Patel, C. M. Kitchen, M. C. Miceli, and J. A. Zack. 2002. Activation of CD8 T cells induces expression of CD4, which functions as a chemotactic receptor. *Blood* 99: 207–212.
67. Zhang, T., R. Somasundaram, K. Berencsi, L. Caputo, P. Gimotty, P. Rani, D. Guerry, R. Swoboda, and D. Herlyn. 2006. Migration of cytotoxic T lymphocytes toward melanoma cells in three-dimensional organotypic culture is dependent on CCL2 and CCR4. *Eur. J. Immunol.* 36: 457–467.
68. Matsumura, S., B. Wang, N. Kawashima, S. Braunstein, M. Badura, T. O. Cameron, J. S. Babb, R. J. Schneider, S. C. Formenti, M. L. Dustin, and S. Demaria. 2008. Radiation-induced CXCL16 release by breast cancer cells attracts effector T cells. *J. Immunol.* 181: 3099–3107.
69. Fong, A. M., L. A. Robinson, D. A. Steeber, T. F. Tedder, O. Yoshie, T. Imai, and D. D. Patel. 1998. Fractalkine and CX3CR1 mediate a novel mechanism of leukocyte capture, firm adhesion, and activation under physiologic flow. *J. Exp. Med.* 188: 1413–1419.
70. Munks, M. W., K. S. Cho, A. K. Pinto, S. Sierro, P. Klenerman, and A. B. Hill. 2006. Four distinct patterns of memory CD8 T cell responses to chronic murine cytomegalovirus infection. *J. Immunol.* 177: 450–458.
71. Böttcher, J. P., M. Beyer, F. Meissner, Z. Abdullah, J. Sander, B. Höchst, S. Eickhoff, J. C. Rieckmann, C. Russo, T. Bauer, et al. 2015. Functional classification of memory CD8(+) T cells by CX3CR1 expression. *Nat. Commun.* 6: 8306.
72. Gerlach, C., E. A. Moseman, S. M. Loughhead, D. Alvarez, A. J. Zwijnenburg, L. Waanders, R. Garg, J. C. de la Torre, and U. H. von Andrian. 2016. The chemokine receptor CX3CR1 defines three antigen-experienced CD8 T cell subsets with distinct roles in immune surveillance and homeostasis. *Immunity* 45: 1270–1284.
73. Glennie, N. D., V. A. Yeramilli, D. P. Beiting, S. W. Volk, C. T. Weaver, and P. Scott. 2015. Skin-resident memory CD4+ T cells enhance protection against *Leishmania major* infection. *J. Exp. Med.* 212: 1405–1414.
74. Jacquelot, N., D. P. Enot, C. Flament, N. Vimond, C. Blattner, J. M. Pitt, T. Yamazaki, M. P. Roberti, R. Daillère, M. Vétizou, et al. 2016. Chemokine receptor patterns in lymphocytes mirror metastatic spreading in melanoma. *J. Clin. Invest.* 126: 921–937.
75. Shin, H., and A. Iwasaki. 2013. Tissue-resident memory T cells. *Immunol. Rev.* 255: 165–181.
76. Wang, D., R. Yuan, Y. Feng, R. El-Asady, D. L. Farber, R. E. Gress, P. J. Lucas, and G. A. Hadley. 2004. Regulation of CD103 expression by CD8+ T cells responding to renal allografts. *J. Immunol.* 172: 214–221.
77. Ely, K. H., T. Cookenham, A. D. Roberts, and D. L. Woodland. 2006. Memory T cell populations in the lung airways are maintained by continual recruitment. *J. Immunol.* 176: 537–543.
78. Wolf, M., and B. Moser. 2012. Antimicrobial activities of chemokines: not just a side-effect? *Front. Immunol.* 3: 213.
79. Cole, A. M., T. Ganz, A. M. Liese, M. D. Burdick, L. Liu, and R. M. Strieter. 2001. Cutting edge: IFN-inducible ELR$^-$ CXC chemokines display defensin-like antimicrobial activity. *J. Immunol.* 167: 623–627.
80. Crawford, M. A., Y. Zhu, C. S. Green, M. D. Burdick, P. Sanz, F. Alem, A. D. O'Brien, B. Mehrad, R. M. Strieter, and M. A. Hughes. 2009. Antimicrobial effects of interferon-inducible CXC chemokines against *Bacillus anthracis* spores and bacilli. *Infect. Immun.* 77: 1664–1678.
81. Stephens, B., and T. M. Handel. 2013. Chemokine receptor oligomerization and allostery. *Prog. Mol. Biol. Transl. Sci.* 115: 375–420. 10.1016/B978-0-12-394587-7.00009-9
82. Salanga, C. L., and T. M. Handel. 2011. Chemokine oligomerization and interactions with receptors and glycosaminoglycans: the role of structural dynamics in function. *Exp. Cell Res.* 317: 590–601.